RESEARCH ARTICLE

An Adaptive Sleep Apnea Detection Model Using Multi Cascaded Atrous-Based Deep Learning Schemes With Hybrid Artificial Humming Bird Pity Beetle Algorithm

SELVARAJ ASWATH[1], (Member, IEEE),
VALARMATHI RAVICHANDRAN SHANMUGA SUNDARAM[1], (Member, IEEE),
AND MIROSLAV MAHDAL[2]

[1]Department of ECE, Veltech Rangarajan Dr. Sagunthala R&D Institute of Science and Technology, Chennai 600062, India
[2]Department of Control Systems and Instrumentation, Faculty of Mechanical Engineering, VSB-Technical University of Ostrava, 708 00 Ostrava, Czech Republic

Corresponding author: Miroslav Mahdal (miroslav.mahdal@vsb.cz)

ABSTRACT Obstructive Sleep Apnea (OSA) is the cessation in breathing that must be identified as early as possible to save the patient's life. Apart from physical diagnosis, a deep learning model can serve the purpose of detecting the apnea swiftly. The detection largely depends upon biological signals such as ECG, EEG, EMG, etc. Because of the high dimensionality nature of the bio signals, feature extraction is very critical in detecting sleep apnea. Many such feature extraction models were fragile to resolve the complexity issue and failed to reduce the non-robustness nature. To surmount all these issues, a novel adaptive deep learning-based model is designed for detecting the sleep apnea. Here two feature sets have been extracted from the ECG signals: Spectral features through Short Term Fourier Transform (STFT) and QRS analysis followed by an auto encoder to extract the deep temporal features. The novel Artificial Hummingbird Pity Beetle Algorithm (AHPBA) is proposed to choose the optimal features and weight parameters, which assists in concatenation of the two feature sets. Then these fused features were given into Multi Cascaded Atrous based Deep Learning Schemes (MCA-DLS) for classification purpose, then it is further optimized by AHPBA by maximizing the variance. MCA-DLS have performed well compared to classifying the signals individually using One Dimensional Convolutional Neural Networks (1DCNN), Long Short-Term Memory (LSTM) and Deep Neural Networks (DNN) as the average accuracy of MCA-DLS is 94.51% whereas the other three provides an average accuracy of 90.83%, 91.98%, and 93.25% respectively for the considered datasets. By using AHPBA the average accuracy of MCA-DLS was enhanced to 96.4%, which is higher than the conventional optimization techniques which are discussed in the result section.

INDEX TERMS Artificial hummingbird pity beetle algorithm, atrous based deep learning schemes, ECG, feature concatenation, feature extraction, STFT, QRS analysis, obstructive sleep apnea.

I. INTRODUCTION

Safe sleep is required to ensure the survival of every individual to maintain better mental and health stability [1], [2], [3]. Some sleep disorders can affect daily activities and routine life. In a human's life, sleep is an essential part to

The associate editor coordinating the review of this manuscript and approving it for publication was Dongxiao Yu.

lead the happy and healthy life. Yet, sleeping disorders have become one of the notable ailments affecting people's lives. One who cannot sleep properly can feel the degradation in the metabolism activities of the body [4], [5], [6]. The most common disorder is sleep apnea, it is a kind of disease where irregular breathing will take place, breathing frequently starts and stops owing the obstruction [7]. Over a full night of sleep, the apnea occurs in the duration of 10 to 30 sec repeatedly up to hundred times. Complete obstruction (Apnea) or partial (Hypopnea) obstruction are the two common types of apneas arise during upper airways [8]. Obstructive sleep apnea (OSA) is a new illness that affects humans more than the other forms of apnea [9]. But failure to detect the apnea disorder tends to create an impact in insomnia and even sometimes it may be fatal. Meanwhile, OSA also causes an exaggerated stage of drowsiness. Further, it ends with increasing stress level, mood swings, lack of memory, car crash, sleep deprivation, heart ailments, etc. [10]. Apnea can be detected using bio signals such as ElectroCardioGram (ECG), ElectroOculoGram (EOG), ElectroMyoGram (EMG), and ElectroEncephaloGram (EEG), which are measured while the patient is sleeping. Polysomnography (PSG) is a kind of study where all these signals are recorded at the same time during the sleep.

With the help of PSG records of one night sleep, the sleep related disorder can be detected. In general, a single record entails 12 numbers of different signals and becomes very expensive to employ [11]. Over the past years, different approaches have been developed to diagnose the apnea disorder with the help of bio signals such as ECG, SpO2 (oxygen saturation), EEG, and air flow activity in the nasal [12], [13], [14]. In contrast with other signals, ECG is widely used to analyze the respiratory activities of humans [15], [16], [17], [18]. Further, [8] and [19] exhibits how an automated model detects the apnea events and identifies its impact on the cardiovascular system by considering Heart Rate Variability (HRV). Nevertheless, the forecasting of OSA by respective signals is a challenging one. Hence, designing an effective computer aided model to screen the sleep disorder [20] is the need of the hour. To achieve this goal, various strategies such as feature engineered machine learning, and deep learning techniques are deployed for detecting the apnea. In feature engineering models, some discriminative features are extracted to perform the detection job [21]. In [15], the models like deep neural network and Hidden Markov Model (HMM) and ECG are employed to do the detection process. Some experts deployed the auto encoder to retrieve the features [22]. Moreover, some more intelligent models are designed with CNN using ECG signals [23], [24], [25]. Recently, researchers have concentrated on utilizing LSTM network to provide the higher results that helps clinicians to diagnose the disease significantly [26], [27]. Using anthropometrics as a valid tool even a GUI was built to detect apnea [28], but it predicts whether a person is having apnea or not only based on body characteristics which is not the most credible data to detect apnea.

The sleep apnea event is identified from an ECG signal by implementing feature extraction methods before subjecting it to detection. Though, the conventional methods use hand crafted features, it still lacks with imprecise results of detection. Different classifiers are used to identify the OSA, yet the required high performance is not obtained due to complexities. Consequently, developing an efficient computer-based model with feature engineering becomes challenging. Deep learning technology can resolve and exploit more detection accuracy to deal with such constraints. The prime intention of deep learning model is to acquire better results by processing signal. In general, the detection system is constructed with preprocessing, feature extraction and classification. Several methods or processes are there to detect sleep apnea, still it faces some challenging issues for further enhancement [29], [30], [31]. Hence, it provokes a need to design a novel deep learning method for diagnosing the sleep disorder.

The core offerings of the developed apnea detection model are summarized below.

Implementation of a novel detection model using optimal feature selection process with multiscale approach of deep learning for diagnosing the sleep disorder accurately and also it helps the practitioner in hospitals to treat the patient's effectively and swiftly.

Development and implementation of a hybridized heuristic algorithm, named as AHPBA, where the traditional Artificial Hummingbird Algorithm (AHA) is superimposed with another algorithm named as Pity Beetle Algorithm (PBA) for tuning the required weights in feature selection and tuning some other parameters such as Hidden Neuron Count, Learning Rate, etc. in classifiers. Thus, it provides an objective of maximizing the accuracy.

Two different feature sets extraction: First set of features (Feature set1) are mainly spectral features and the second one (Feature set2) is temporal, which is extracted after a QRS analysis followed by an autoencoder. The final temporal features extracted from the autoencoder consists of the most noteworthy features of data which is free of noise. These two are then further integrated with each other and with the help of optimal weights. This integration and upgradation of optimal weights is done by Artificial Hummingbird Pity Beetle Algorithm (AHPBA).

An adaptive classifier model, termed as MCA-DLS, in which the classification is subjected to cascaded 1DCNN, LSTM and DNN. Here, the parameters like learning rate, epochs, batch size and hidden neuron count are tuned optimally by AHPBA algorithm, to reach the expected detection results with less complexity.

Analyzation of the experimental results using divergent factors with a few recent conventional optimization algorithms and classifiers.

II. LITERATURE REVIEW
A. RELATED WORKS
In 2022, Zarei et al. [15] have illustrated the novel detection model using a hybrid deep learning model. Initially,

the source signals were gathered and had been subjected to preprocessing. In CNN network model, the fully connected layers were used to diagnose the disorder. Further, Apnea Hypopnea Index (AHI) was considered to distinguish the apnea events from signal. The simulated results were validated by extracting the signals from UCDDB (University College Dublin Data Base) and ECG datasets. The performance was measured with divergent parameters and its respective results were compared with other existing algorithms. Though it provides good results the complexity in size is the big issue to deal with.

In 2021, Álvarez et al. [32] have designed the new approach of using deep learning for detecting sleep disorders. Here the oxygen level of every individual was taken into account for detection purpose. For experimentation, 3196 counts of SpO2 signals were fetched. At first, the acquired signals were trained in CNN using 859 subjects that detected the apnea events during sleep. To get the optimal values, the parameters in CNN were optimally chosen by Bayesian optimization. Though technically the system may be good but with only SPO2 we can't predict OSA as SPO2 values varies with different illness as well.

In 2021, Liu et al. [33] demonstrated the Weighted Loss Time Dependent (WLTD) and multiple scale dilation attention 1-D CNN for OSA identification. The dilation-based convolution operation was mostly used to balance the parameters and performance. Subsequently, weighted features were chosen and applied in attention mechanism to increase the detection efficiency. Further, the classification was performed with weighted cross entropy loss function and HMM to conquer the class imbalance issue, which has paved the way for further enhancement. Finally, distinct metrics were considered to compute the significant performance analysis that detected the apnea events.

In 2021, Rabbi et al. [34] have utilized ECG signal to identify the OSA using scalogram assisted SCNN. In order to get the scalograms of signal, the Continuous Wavelet Transform (CWT) was applied for transformation. Subsequently, an Empirical Mode Decomposition (EMD) was emerged with finding the correlation in Intrinsic Mode Functions (IMFs), in which the CWT was included to acquire the hybrid scalograms. With the help of features, the training and testing were performed by CNN. The validation was done based on heterogeneous parameters and compared with traditional models, but the SCNN based OSA detection models has a low generalization capability.

In 2022, Gupta et al. [16] have framed the novel approach of Smoothed Gabor Spectrogram (SGS) by ECG to identify the sleep apnea. The spectrogram features of input signal were given as input to priorly trained model such as ResNet50, SqueezeNet and also to their deep learning model termed as OSACN-Net. The proposed model has analyzed the performance by varying the 10-fold cross validation. In contrast with ResNet50 and SqueezeNet, the suggested OSACN-Net has exhibited greater results that have resolved the computation complexity. Compared with

former approaches, this model has attained the high expected accuracy value, but in this method false acceptance rate is also high. In 2022, Wang et al. [35] have designed the automated model of Bi-directional LSTM (Bi-LSTM) for detecting sleep disorder using EEG recordings with the aid of SAS equipment. Here, 42 different subjects were taken for training purposes with PSG recordings. Tenfold cross and Adam optimizer was used to optimally enhance the performance Hence, the outcome has revealed that it has maximized the performance regarding accuracy and precision. The time complexity is too high since different bio signals were taken into account apart from ECG.

In 2021, Pedram et al. [10] have implemented an innovative method for identifying the apnea activities. This method was composed of feature extraction and selection, followed by classification. The ten different time domain features were extracted, which were mitigated to five numbers of features. To achieve this, two techniques, such as Discriminant Linear Analysis (LDA) and Principal Component Analysis (PCA) were adopted. Here, Random Forest (RF) classifier, Decision Tree (DT) and SVM were considered to classify the signals into normal or abnormal. Here the basic classifiers alone were used to classify the signal. No deep learning techniques were justified.

In 2021, Bozkurt et al. [36] have framed the novel hybridized model of machine learning techniques by using ECG signals for sleep wake stages. Among 10 apnea affected patients, HRV was taken to evaluate the performance. Using filtering model, the QRS wave component was determined with ECG signal source. For experimentation, they have considered 9 signals, in which 25 distinct features were obtained, thus it has resulted with 225 features. Further to reduce the dimension of features, principal component analysis and fisher feature selection were used. Consequently, these reduced features were fed into KNN, SVM, DT and ensemble models. Therefore, the performance was computed with accuracy, sensitivity and specificity measures. After analyzing the model, it was proved that it has improved the desired level of detection rate to diagnose the disease. Here the limitation is the model does not take much care on the noise that affects the ECG signal and the high training cost.

B. PROBLEM SPECIFICATION

The detection of OSA using ECG is non-invasive and it requires wearable mobile device and the cost required for the implementation is high. However, it is difficult to analyze the non-stationary sympathetic nerve signals from the ECG signal, and also the heart rate variability from the patients. Therefore, to analyze the large dimensional data with reduced cost, many deep learning based approaches were developed and the features & challenges of those approaches are discussed below. CNN and LSTM [37], [38], [39] reduce the computation overload and it increases the robustness of the apnea detection system and it effectively handles the large dimensional data. But it has high intrusiveness and limited

availability. In addition, it does not fulfil the generalization capability. CNN [40], [41] dynamically enhanced the diagnostic ability of the oximetry signal and also it includes the capability of the screening in the OSA detection system. Nevertheless, it only considered the SpO2 parameter alone, other parameters like API and central apnea index are not focused in the OSA detection system. Furthermore, the reliability of the system is very poor. 1D-CNN [42], [43] decreases the time complexity and the computation cost. In addition, it can identify the complex patterns in the original data. Yet, it requires a large training dataset for the detection of OSA. But it has high variability in the scoring of PSG. SCNN [34] provides very high stability of the system. Moreover, it effectively improves the imbalance problem and classification performance with reduced computation complexity. Consequently, it is highly sensitive to errors and therefore, the generalization capability is low in the SCNN-based OSA detection approach. OSACN [16] automatically and very effectively extracts the network features for increasing the adaptability. Even though the false acceptance rate is excessively high, it also minimizes the loss that occurs in the OSA detection system. But it needs more space for recording the health patterns in the OSA detection system. Bi-LSTM [35] has low load, high recognition rate, and high-efficiency in the OSA detection. Therefore, it gives high sensitivity, selectivity and f-measure. However, it does not ensure the security and authenticity of the health information. Nonetheless, it is very difficult to implement, and it is a time-consuming process. PCA [36] effectively decreases the dimensionality for improving the classification accuracy. Further, the abnormal events of the patients are accurately detected. But the ECG signal is highly affected with white Gaussian noise and the salt & pepper noise; Therefore, it requires further improvement in the system adaptability. These challenges in the existing OSA detection approaches are required to be resolved by the newly suggested deep learning based OSA detection approach. Therefore, the new OSA detection approach should enhance the performance of the model by extracting the meaningful features while reducing the noise in the features, enhance the accuracy and to be robust to different ECG data.

III. DESCRIPTION OF PROPOSED ARCHITECTURE AND EXPERIMENTED DATASET

A. DATASET DETAILS OF SLEEP APNEA DETECTION

Here two different datasets with ECG signals were considered. Mostly for medical related illness MRI or CT images [26], [27] will be considered for detecting the disease. But in some, even the microscopic images were also considered [28], but those can't be used in detecting apnea, as apnea tends to occur for several minutes to several hours and it may repeat several times within a night of sleep. Hence here two distinct data sources related to ECG are considered and the same are described as follows.

Dataset 1: The Apnea-ECG database can be accessed through the below link https://www.kaggle.com/datasets/

ecerulm/apneaecg; (https://physionet.org/content/apnea-ecg/1.0.0/) Accessed Date: 2022-10-29. It includes around 70 ECG signals related

to sleeping stage. The signals are in nature of 16 bits/sample, where each pair entails 100 samples/second. It contains both training (35) and testing data (35) to find out whether the apnea is present or not. For each training file, an annotation file was also there which had been annotated by human experts regarding whether apnea was there or not for each minute of recording.

Dataset 2: The second dataset can be accessed through the following link https://www.physionet.org/content/slpdb/1.0.0/: It is also termed as MIT-BIH Polysomnographic Database. It is the congregation of physiological sleep signals. Totally, this database constitutes 18 signal records along with four files.

The original signals were fetched from the above two links and it is denoted by S_a, where $a = 1, 2, \ldots, A$; in turn A annotates the total number of collected sleep signals. Figure 1 depicts the sample sleep signals for both datasets.

B. ARCHITECTURE DETAILS OF SLEEP APNEA DETECTION SYSTEM

All the conventional processes have been using the PSG recordings for detecting the sleeping disorder. Despite promising results, it still requires more development to get an effective result. To overcome some issues like time consumption, cost expenses, reliability, etc., learning methods occupy the frontline position to forecast the disease. In the first hand, machine learning approaches have been utilized to achieve greater results. But it exists with performance degradation as PSG or ECG signal contains some noisy features and slow in process. This becomes difficult for practitioners to diagnose the disease in a significant way. Also, various sensors are used to receive the signal, but it is vulnerable if such unwanted noises intrude the ECG signal. To help with further enhancement, deep learning models have been deployed for apnea detection. Sometimes, the manual calculation of signal recordings can mislead the detection process. Deep learning techniques such as CNN, ANN are commonly used; however, it stumbles to maximize the accuracy value by considering the large dimensional feature sets. By addressing such issues, a novel adaptive based deep learning model with hybrid heuristic approach for sleep apnea detection has been designed, which is elucidated in Figure 2.

The proposed model possesses distinct stages as (a) Signal

$$v = \left(\frac{\text{wtFt} - \text{btFt}}{\text{btFt}} \right) \tag{1}$$

collection, (b) Feature extraction (c) Weighted features and (d) Detection. In the first stage, the input raw signals are fetched from two different data sets for subsequent sections. On the second stage, the extraction is carried out by two ways. (i) The gathered signal is fed into de-composition by using STFT, which is then further used to retrieve the spectral features of decomposed signal, these features are
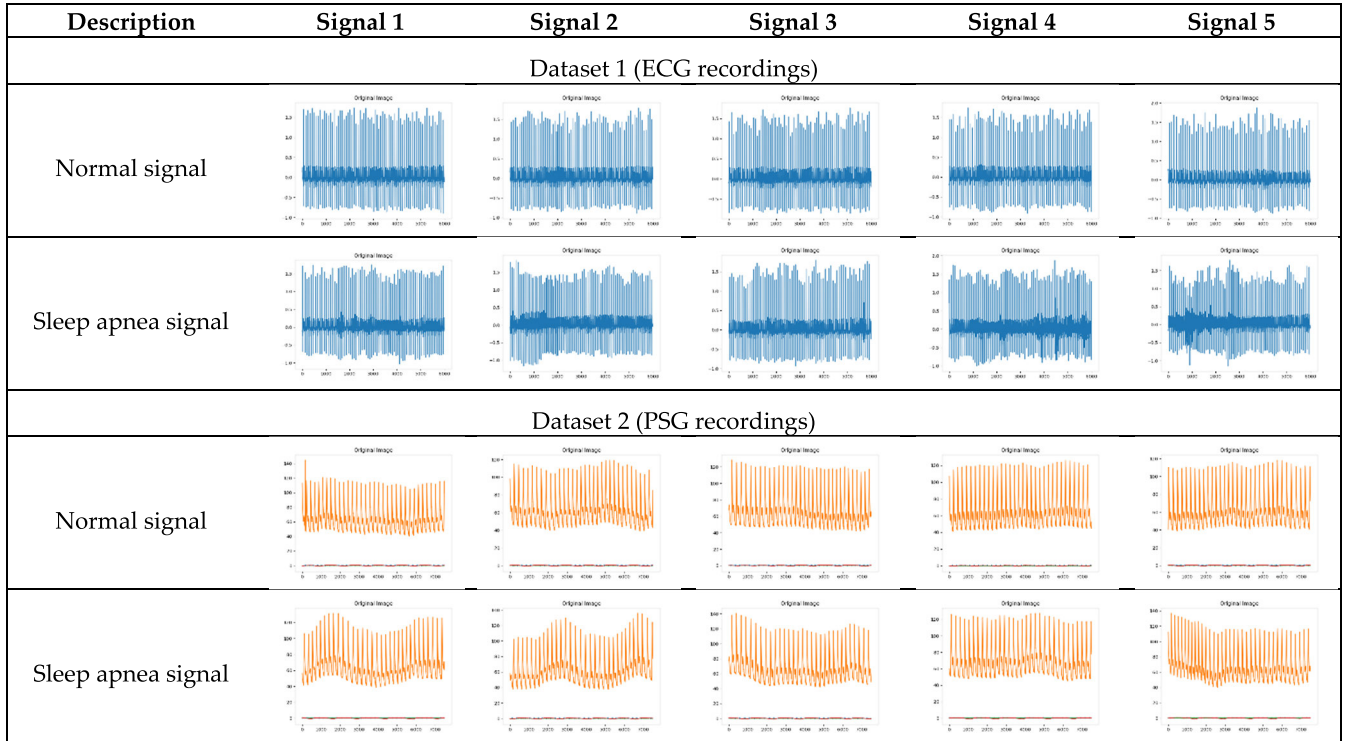
Description	Signal 1	Signal 2	Signal 3	Signal 4	Signal 5
Dataset 1 (ECG recordings)					
Normal signal					
Sleep apnea signal					
Dataset 2 (PSG recordings)					
Normal signal					
Sleep apnea signal					

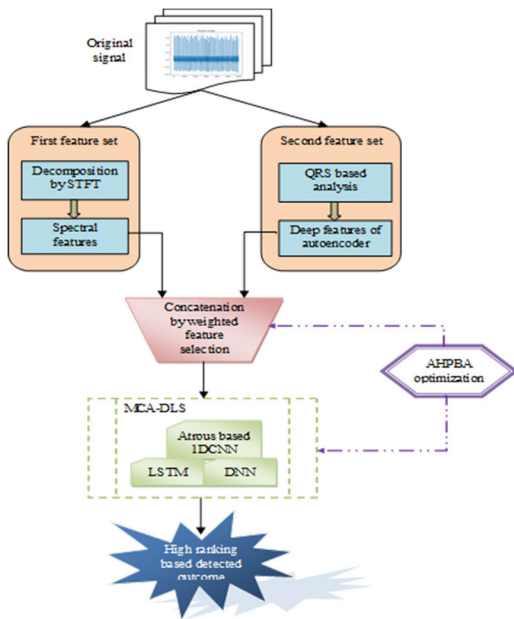**FIGURE 1.** Sample signals of normal and apnea signals.

FIGURE 2. Schematic representation of proposed sleep apnea detection using adaptive deep learning model with hybrid algorithm.

called as first feature set. (ii) The input signal is given to QRS analysis that is followed by autoencoder to extract the deep features which is used to determine the relevant features than noisy signal features to enhance the performance and it is termed as second feature set. Subsequently, these resultant features are fused together with the help of selecting optimal

features and weight factor. It is achieved by using the proposed Artificial Hummingbird Pity Beetle Algorithm (AHPBA) to reduce the dimensional issue and to increase the variance among the signals. Finally, the weighted features are given into Multicascaded Atrous based Deep Learning Scheme (MCA-DLS). It is a proposed novel ensemble classifier, that comprises of 1DCNN, LSTM and DNN, where the final outcome is computed by averaging method. In order to attain the optimal values of such parameters, the proposed AHPBA is employed for tuning the hyper parameters such as hidden layers, epochs, etc. that evades performance degradation. Due to this parameter optimization, it mitigates the complexity and further maximizes the accuracy rate. Hence, a comparative performance is evaluated across divergent parameters and ensures that it provides the appropriate results for diagnosing the sleep disorder (OSA) of humans.

IV. SIGNAL FEATURE EXTRACTION AND OPTIMAL FEATURE SELECTION WITH META-HEURISTIC ALGORITHM FOR SLEEP APNEA DETECTION

A. PROPOSED AHPBA

The proposed AHPBA is primarily used for tuning the parameters that are required for obtaining the features and classifying the signals. It is developed as a hybrid manner by incorporating two algorithms as AHA and PBA. The advantages of using these two algorithms are: these two algorithms containing less computation complexities, high convergence rate, handles the single objective model, etc. The proposed algorithm is mainly used for two purposes:

1. In feature fusion, during the weighted feature selection phase, the weights are tuned using the AHPBA and subsequently the features optimally selected. 2. In the proposed classification model MCA-DLS, various parameters such as the hidden neurons of 1DCNN and LSTM, learning rate of both 1DCNN and DNN, epochs in LSTM and batch size of DNN are optimally determined by using AHPBA to get the effective classification results.

In the proposed algorithm, the vector in traditional AHA is considered to determine the ability of hummingbird to get the prey. Since it represents the arbitrary value, it does not support all the scenarios. Hence, the vector can be newly modelled by using Equation (1).

It defines the condition with worst fitness and best fitness as wtFt and best fitness as btFt, if $v < 0.5$ then the best solution is accomplished by AHA, otherwise, it is done by using PBA. The vice versa condition was also tried and from experimenting it is concluded that to follow AHA if $v < 0.5$, else to follow PBA. The following figure justifies the condition set for the proposed model.

In Figure 3.a and 3.b it is clearly visible that the cost function arrived using AHPBA is pretty low compared to that of all heuristic algorithms and also it is low compared to

(a)

(b)

FIGURE 3. Convergence of cost function of the different heuristic algorithms for both the datasets.

the proposed algorithm been executed in vice versa condition (i.e the best solution is accomplished by AHA if $v > 0.5$, otherwise, it is done by using PBA, which is mentioned as PBAAH. The two algorithms: artificial hummingbird and pity beetle are explained as follows.

AHA [47]: The AHA does the optimization by the natural behaviour of hummingbirds. It mainly includes three elements such as food sources, population (No. of hummingbirds) and visit table. When coming to the foraging state, it again includes with three different strategies as guided foraging, territorial foraging, and migrating foraging. The mathematical formulation is given below.

Step 1: Initialization: - Consider h numbers of birds and prey for optimization. It is randomly initialized and represented in Equation 2.

$$f_j = \text{LB} + n \cdot (\text{UB} - \text{LB}), \quad j = 1, 2, \dots, h \quad (2)$$

Term, UB and LB refers the upper and lower boundary values, n is the random number contains the range as [1, 0]. The visit table is defined here as the visit level of every food for corresponding birds. Simply, it depicts how much time it gets visited by bird. More visit level gives more priority. Henceforth, every bird attacks the food with the help of the visit table.

The food sources are initialized in visit table is given in Equation (3).

$$st_{j,k} = \begin{cases} 0 & if\ j \neq k \\ null & j = k \end{cases}, \quad j, k = 1, 2, \dots, h \quad (3)$$

Here, null means the food is taken by hummingbird, then the value 0 represents that k^{th} food is visited by j^{th} bird.

Step 2: Guided searching: - This behaviour is mimicked by considering the more visit level of food sources. Once the food is targeted, the hummingbirds fly to feed it. The flight or flying nature depends on three directions such as omni-directional, diagonal, and axial flights. These three patterns are modelled using the Equation (4), Equation (5) and Equation (6).

$$G_{af}^{j} = \begin{cases} 1 & \text{if } j = \text{rdj} ([1, z]) \\ 0 & \text{otherwise} \end{cases} \quad j = 1, \dots, z \quad (4)$$

$$G_{df}^{j} = \begin{cases} 1 & \text{if } j = D(k), k \in [1, i], \\ & D = \text{rdp}(i), \\ 0 & i \in [2, (n_1 \cdot (z - 2)) + 1] \\ & \text{otherwise} \end{cases} \quad j = 1, \dots, z \quad (5)$$

$$G_{of}^{j} = 1 \quad j = 1, \dots, z \quad (6)$$

In the aforementioned equations, the arbitrary generation of random integers and permutation integers are indicated by rdj ([1, z]) and rdp (i), respectively. Further, the random values are considered from 0 to 1 using the variable n_1. With the help of these flights, a candidate food source is acquired.
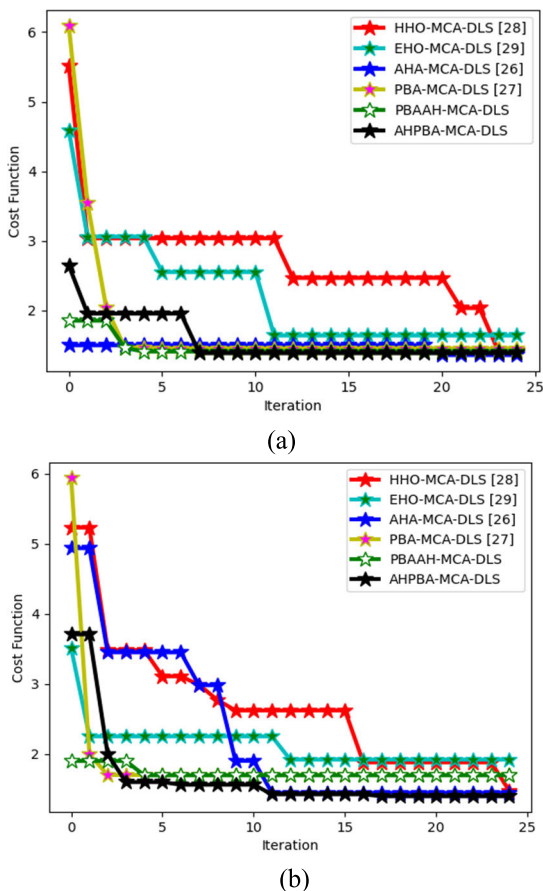
Based on this, prey can be updated from older position to another position. It is evaluated using Equation (7).

$$g_j(b+1) = f_{j,\text{tg}}(b) + \alpha \cdot G \cdot \left(f_j(b) - f_{j,\text{tg}}(b)\right) \quad (7)$$

Here, the position of prey and targeted prey is declared by $f_j(b)$ and $f_{j,\text{tg}}(b)$, respectively. Then, the guided factor as $\alpha \sim R(0, 1)$ signifies the normal distribution function with mean as 0 and standard deviation as 1. Finally, the position of food source is upgraded with fitness value FT $(\cdot)$. It is shown in Equation (8).

$$f_j(b+1) = \begin{cases} f_j(b) & \text{FT}\left(f_j(b)\right) \leq \text{FT}\left(g_j(b+1)\right) \\ g_j(b+1) & \text{FT}\left(f_j(b)\right) > \text{FT}\left(g_j(b+1)\right) \end{cases}$$
$$(8)$$

Step 3: Territorial searching: - Once after the target prey is visited that has been eaten already. Then, the hummingbird is likely to visit new or another food source in their own territory. Based on territorial region, the new position is generated using Equation (9).

$$g_j(b+1) = f_j(b) + \beta \cdot G \cdot f_j(b) \quad (9)$$

Term, β specifies the territorial factor derives by $\beta \sim R(0, 1)$.

Step 4: Migration searching: - The frequent visiting lacks the food sources in respective region. A migration coefficient is taken to consider the worst nectar-refilling rate. With this rate, it migrates into a new prey. Hence, it again presumes the arbitrary generation of food source with worst nectar. It is derived by Equation (10).

$$f_{\text{wrst}} = \text{LB} + n \cdot (\text{UB} - \text{LB}) \quad (10)$$

Thus, the optimal solution is obtained from AHA that used for optimizing the parameters.

PBA [48]: The bark beetles are considered as the population for optimizing the solution. It inspires by the process of reproduction. It mainly comprises three steps as initialization, new hyper-volume selection pattern and update population position, which are explained as below.

Step 1: Initialization: - Arbitrarily, the population are initialized with the generation of Random Sampling Technique (RST) otherwise called as random position technique (RPT). Here, the male beetles are named as pioneer which are otherwise also known as pioneer particles. Each particle is defined with lower bound, upper bound, dimensional vector and also total populations. It is given in Equation. (11).

$$y_x^{(0)} = rpt\,[Lb, Up, V, P] \quad (11)$$

where, $Lb = [Lb_1, \ldots, Lb_V]$, $Ub = [Ub_1, \ldots, Ub_V]$
$x = 1, 2, \ldots, P$

Here, the lower and upper bound value is noted by Lb and Ub, respectively and also determines the total population and dimensional vector is denoted as P and V, correspondingly.

Step 2: Selection pattern of new hyper-volume: - To select the new values, a search space is created with respect to particles. Therefore, based on each pattern, new particles of pioneer are randomly positioned using Equation (12).

$$y_x^{(n)} = \text{rpt}\left[lb^{(n)}, up^{(n)}, V, P\right] \quad (12)$$

where, $\left[\text{lb}_k^{(n)}, \text{up}_k^{(n)}\right] \in \left[y_{\text{bt,k}}^{(n)} \cdot (1 - p_f), y_{\text{bt,k}}^{(n)} \cdot (1 + p_f)\right]$

Term, $y_{\text{bt,k}}^{(n)}$ refers the birth position vector, pattern factor as p_f and n defines the generation.

Neighbouring search hyper-volume: Assume the neighbouring factor nb_f, it determines the parameter area. It lies in the range of 0.01 and 0.20. It is formulated using Equation. (13).

$$y_{\text{bt}}^{(n+1)} = \begin{cases} y_{\text{bt}}^{(n)}, & \text{if } F\left(y_{\text{bt}}^{(n)}\right) < F\left(y_{x,z}^{(n)}\right), \\ y_{x,z}^{(n)}, & \text{else} \end{cases} \quad (13)$$

In the above Equation, the birth position and new position is indicated by $y_{\text{bt}}^{(n)}$ and $y_{x,z}^{(n)}$, respectively. Here, the term z varies from 1 to total number of broods.

Mid-scale search hyper-volume: The mid-scale factor ms_f is taken for creating the best solution. It has the value of 0.1 and 1.

Large-scale search hyper-volume: The large-scale factor ls_f contains the value of 1 and 100 used for updating the position.

Global-scale search hyper-volume: It assumes unsuccessful function evaluations as fe_u and total function evaluations as fe_{tot}. It contains the value of 0.05 and 0.25.

Memory search hyper-volume: It is used to select the memory (Me) to enhance the robustness of model. Here, it presumes the tuning factor tu_f that is more equal to value of 0.005 and 0.05.

Step 3: Population updating: - The position of mating males and females are updated. While updating, the existing broods are expired, and new position is generated with birth places. Hence, it is modelled using Equation (14).

$$y_{x,z}^{(n)}$$
$$= \begin{cases} \text{rpt}\left[y_{bt,k}^{(n)} \cdot (1 - nb_f), y_{bt,k}^{(n)} \cdot (1 + nb_f), V, P\right], \text{if } z = 1 \\ \text{else} \\ \begin{cases} \text{rpt}\,[Lb, Up, V, P], \text{if } fe > fe_u \\ \text{else} \\ \begin{cases} \text{rpt}\left[y_{bt,k}^{(n)} \cdot (1 - ms_f), y_{bt,k}^{(n)} \cdot (1 + ms_f), V, P\right] \\ \text{if } f\left(y_{x,z-1}^{(n)}\right) < f\left(y_{bt}^{(n)}\right) \\ \text{else} \\ \begin{cases} \text{rpt}\left[y_{bt,k}^{(n)} \cdot (1 - ls_f), y_{bt,k}^{(n)} \cdot (1 + ls_f), V, P\right], \\ \quad\quad \text{if } t < s \\ \text{Me, otherwise} \end{cases} \end{cases} \end{cases} \end{cases}$$
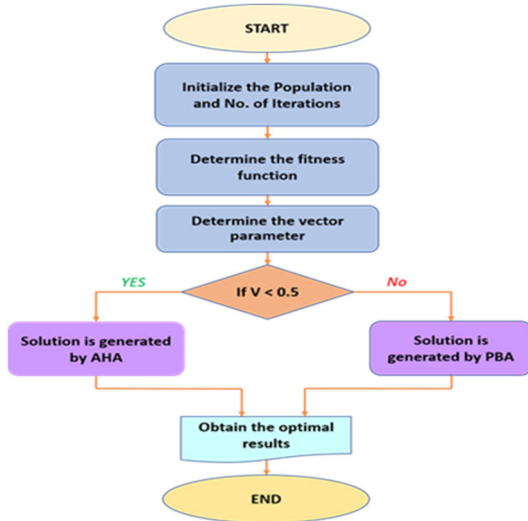$$(14)$$

The detail of PBA is exhaustively covered in [48].

FIGURE 4. Flow chart of the proposed optimization model (AHPBA).

The pseudo code of novel AHPBA is given below.

Algorithm 1 Suggested AHPBA

Assume the total population and maximum iteration count
Determine the fitness function.
Define the condition with vector v using Equation (1)
Perform while condition
   Check if $v < 0.5$
     Then the solution is generated by AHA
        Using Equation (2), initialization is processed.
        Execute guided searching with Equation (8)
        Execute territorial searching with Equation (9)
        Execute migration searching with Equation (10)
Else
    The solution is generated by PBA.
      Initialization is done by Equation (11).
      New hyper-volume is generated.
      Using Eq. (14), the population is updated.
    Terminate if
    Returns the finest solution
Terminate while
Acquires the optimal rate and values.

B. TWO LEVEL FEATURE EXTRACTION

Once the required signals are collected, they are subjected to a two-stage feature extraction. It is briefly described in the following sub sections.

1) FIRST LEVEL EXTRACTION PROCESS

The extraction is accomplished by decomposing the signal with STFT and then the decomposed signal is used for extracting the spectral features.

STFT [49]: Short term Fourier Transform (STFT) is used to decompose the signal. Here, the input signal S_a is given to STFT. Compared to other transforms STFT is simpler to implement and it is more advantageous when rendering powers. By using this transform the spectral centroids can be easily find and these centroids can be used to extract the meaningful features of the given signal. As the input is in the form of signal, the foremost step is to determine the trade-off level between frequency and time domain traits. Hence, the input signal is decomposed into its respective frequency component via Equation (15).

$$D(\omega) = \int_{-\infty}^{\infty} S_a(n) p^{-i\omega n} dn \qquad (15)$$

Simultaneously, the time characteristic of signal is defined by Discrete Fourier Transform (DFT) in Equation (16).

$$T(m) = \sum_{k=0}^{K-1} S_a(k) L_K^{km} \qquad (16)$$

Here, the discrete time and frequency index is indicated by k and m, and also the total number of samples is given by K. Further, L_K^{km} defines the transformation kernel function, expressed in Equation (17).

$$L_K^{km} = e^{\left(-i\left(2\pi km / K\right)\right)} \qquad (17)$$

Hence, the STFT based signal is attained and denoted by S_a^{dec}. From this signal the spectral features are extracted. Spectral features: The decomposed signal S_a^{dec} is fed as input to spectral feature extraction process. The spectral feature is mainly useful for determining the most sensitivity features of both power and frequency of decomposed signal. Here, the spectral feature is calculated by spectral centroid. Other than the other spectral moments, the centroid moment acquires the resultant noise-resistive features which changes with time. It will indicate the frequency at which the energy of a spectrum is centred upon. The spectrum elements decomposed from the signal are evaluated by using the Eq. (18).

$$SF = \frac{\sum_c M(c) y(c)}{\sum_c M(c)} \qquad (18)$$

Term, $M(c)$ and $y(c)$ annotates the spectral magnitude and frequency of signal. Further, the term c is the total number of samples in STFT signal. Therefore, the first feature set is obtained and noted as Fe^1. A total of 10500000 and 45978273 features are extracted as spectral features from dataset1 and dataset2 respectively.

2) SECOND LEVEL EXTRACTION PROCESS

The second feature set is acquired by processing the signal through QRS analysis and deep features extraction through autoencoder.

QRS analysis: From the input signal S_a, it analyses the Q-wave, R-wave and S-wave. Over the signal, the first negative wave is designated as the Q-wave. Then, R-wave represents the positive waves in signal and finally, S-wave represents the negative wave right after the occurrence of positive wave. In this QRS analysis the peaks have been found out for the entire signal. Based on this analysis, the QRS signal peaks have been found out and denoted as S_a^{QRS}.

Autoencoder [50]: It infers from neural network model that performs with both encoder and decoder. The prime intention of this model is to determine the deep features of QRS based signals (S_a^{QRS}), which are free from noise. As the name implies, it poses two blocks to estimate the relevant features. The key point of using autoencoder is to acquire the features in denoised manner. It will reduce the number of peak values as some of it might be fake one or noisy one. The process of autoencoder is done by three major layers like input, output, and hidden layers.

In the first hand, the encoder block integrates the latent characteristic features of QRS signal S_a^{QRS} that process with hidden layer. It is represented using Equation (19).

$$\text{AE}_\text{H} = \gamma \left(\Im \left(S_a^{QRS} \right) \right) \tag{19}$$

After performing the hidden function, the decoder will decode the information as per the Equation (20).

$$\text{AE}_O = \gamma \left(\Im \left(\text{AE}_\text{H} \right) \right) \tag{20}$$

Finally, to estimate the deep features, it requires computing the loss function among the layers of input and output, which is given in Equation (21).

$$\text{ls} = \| \text{AE}_O - \text{AE}_\text{H} \|_2 \tag{21}$$

Therefore, the extracted deep feature is also known as second feature set that is marked as $\text{Fe}^{(2)}$. A total of 2100000 and 1019700 R-peaks are extracted using QRS analysis followed by autoencoder from dataset1 and dataset2.

C. OPTIMAL FEATURE SELECTION

Since both the feature set contains the beneficial traits and different lengths, it needs to be combined with each other. Initially, the optimal features are selected from two sets separately, because of this selection the dimensional issue can be resolved which helps in reducing the computational complexity. The selection of optimal features is helpful to mitigate the occurrence of falsely chosen features and evade from the performance degradation. Thus, the optimal features are determined by influencing the proposed AHPBA. Hence, the optimal selected features for both set is noted by Fe_opt^1 and $\text{Fe}_\text{opt}^{(2)}$. Subsequently, these two features are fused together by taking the weight factors. As the features are in optimal representation, the weight is also required to determine optimally to prevent the degradation. Again, the optimal weights can be estimated by using novel AHPBA. The mathematical expression of optimal feature selection and fusion is shown in Equation (22).

$$\text{FC}_f^{wt} = \left(W_1 * \text{Fe}_\text{opt}^1 \right) + \left(W_2 * \text{Fe}_\text{opt}^{(2)} \right) \tag{22}$$

By optimal selection, it aids to increase the variance among the signals that is illustrated as objective function in Equation (23).

$$\text{OF}(1) = \underset{\{W_1, W_2 \text{Fe}_\text{opt}^{(1)}, \text{Fe}_\text{opt}^{(2)}\}}{argmax} [Var] \tag{23}$$

Here, the two weights W_1 and W_2 lies in the range of [0.01 to 0.99]. Similarly, the optimal features, $Fe_\text{opt}^{(1)}$ and $Fe_\text{opt}^{(2)}$ that varies from 1 to 10 for each set. Further, the term *Var* refers the variance, which is defined by a measure of how data points differ from the mean value. It is computed using Equation (24).

$$Var = A \left[(Y - \mu)^2 \right] \tag{24}$$

Here, the given signal and mean is denoted by Y and μ, accordingly. Figure 5 depicts the optimal feature selection for concatenating the features using AHPBA. Finally, a feature size of 856700 and 948732 was obtained as the optimal weighted features for the dataset 1 and dataset 2 respectively.
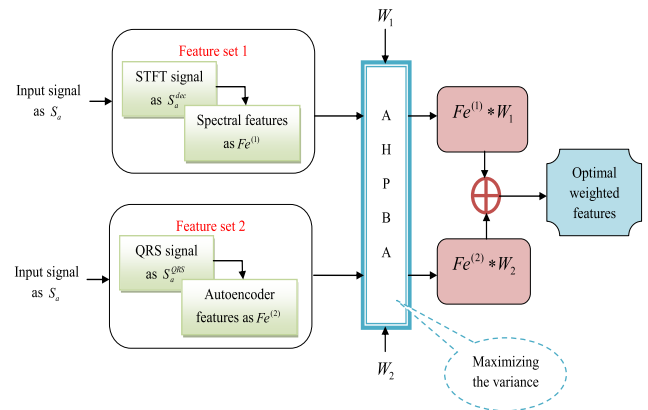

FIGURE 5. Process of obtaining optimal weighted features using AHPBA approach.

V. INTELLIGENT SLEEP APNEA DETECTION SYSTEM USING MULTI-CASCADED ATROUS-BASED DEEP LEARNING SCHEMES

A. 1D-CNN

The 1DCNN [33] model is employed here for classification purpose. Since the source is in signal format, one dimensional based learning model is more than enough for classification task. Thus, 1DCNN is utilized for accomplishing the objectives. The structure of 1DCNN is composed of many layers such as convolutional layer, fully connected Multilayer Perceptron (MLP) consisting of hidden layer, softmax output layer and max pooling layer. Here, the input is taken as weighted features FC_f^{wt}, which is fed into 1DCNN model, the input layer passes the features to single convolutional layer. In this layer, the convolution operation is done by using the series of filters. Further, this filter (kernel) helps to make the feature map by convolving the signal features to acquire the appropriate results. Therefore, the convolution operation and kernel function is expressed using Equation (25).

$$Cn_s = Af \left[\sum_{s=1}^{S} FC_s^{wt}(l) * k(l) + b(l) \right] \tag{25}$$

Here, S defines the total number of samples, l refers the convolution layer and b refers the weight. Meanwhile,

Af $(\cdot)$ signifies the activation function. The resultant output from the above layer is given as input the next MLP layer to classify the features further. In this, the hidden layer is mainly computed with Rectified Linear Unit (ReLU) function. It performs on the basis of non-linear function and it is derived via Equation (26).

$$Af\left(Cn_s\right) = \max\left(0, Cn_s\right) \tag{26}$$

Finally, the output layer provides the classified signal results. The diagrammatic representation of 1DCNN method is depicted using Figure 6.
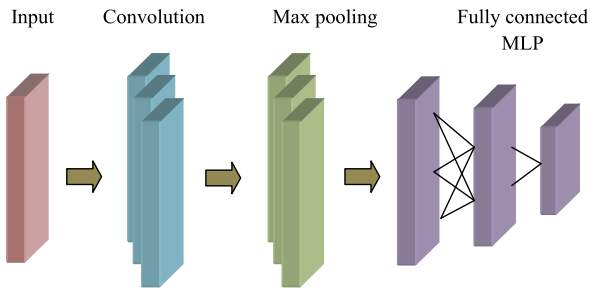
FIGURE 6. General structure of 1DCNN model.

B. LSTM

To process the LSTM [15] model, the optimal weighted feature FC_f^{wt} is taken as input. The major objective of LSTM model is to counteract the confined matters of time dependency of signal. Thus, the LSTM is an advantageous variant of RNN network. In contrast with other networks, it has the potential to rectify the gradient vanishing problem. The weighted features of signal are classified by determining the signal variations to obtain the results as normal or apnea signal. It builds with three major gates such as forget gate fg, input gate ig, and output gate og. The mathematical functionalities of LSTM are given by below equations.

$$fg_a = \lambda_{fg}\left(u_{fg} \cdot FC_f^{wt} + v_{fg} \cdot hn_{a-1} + bi_{fg}\right) \tag{27}$$

$$ig_a = \lambda_{ig}\left(u_{ig} \cdot FC_f^{wt} + v_{ig} \cdot hn_{a-1} + bi_{ig}\right) \tag{28}$$

$$og_a = \lambda_{og}\left(u_{og} \cdot FC_f^{wt} + v_{og} \cdot hn_{a-1} + bi_{og}\right) \tag{29}$$

$$s_a = fg_a \cdot s_{a-1} + ig_a \cdot \lambda_c\left(u_s \cdot FC_f^{wt} + v_s \cdot hn_{a-1} + bi_s\right) \tag{30}$$

$$hn_a = og_a \cdot \lambda_h\left(s_a\right) \tag{31}$$

Term, λ specifies the hyperbolic tangential function of LSTM, the weight factor is represented by u and v, respectively. The previous hidden state is noted by hn_{a-1} and the bias term as bi. The general architecture of LSTM is demonstrated in Figure 7.

C. DNN

The DNN [51] is most essential learning approach in signal processing. It is used here to classify the features into affected and non-affected signals of sleep apnea. Like other models,
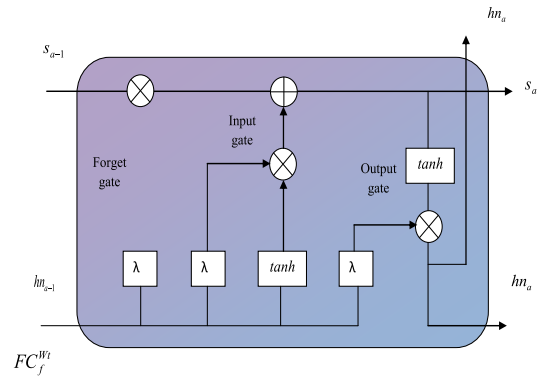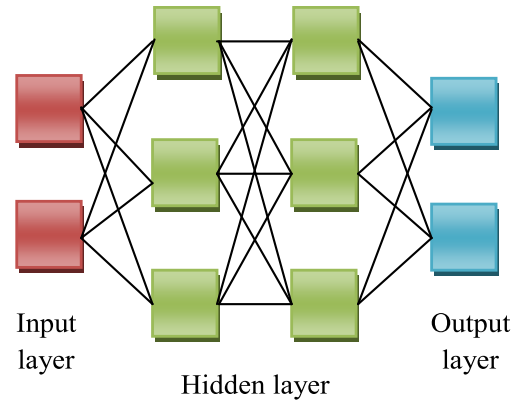
FIGURE 7. LSTM network architecture.

FIGURE 8. DNN structure.

it constitutes three layers as input, output and hidden layer, where it constructs many hidden layers with myriads hidden units. The weighted feature FC_f^{wt} is fed into the first layer of input layer in DNN. It is followed by hidden layer that comprises with weight and bias term to process the signal features. Also, some activation functions are also entailed in training and testing process to acquire the appropriate results. The main benefit of DNN is that it can also learn the features of unlabelled, unstructured signals. Thus, from the output layer, the classified outcome is obtained for detection. Figure 8 elucidates the DNN structure.

D. MULTI-CASCADED ATROUS-BASED DEEP LEARNING SCHEMES

The MCA-DLS is newly proposed to attain the final classified results. Since the optimal features are given in large-scale manner, the single convolution layer does not support to acquire the expected classified value. It also tends to mitigate the performance enhancement and robustness of system. To overcome such issues, atrous (dilated) convolution layers are included in the 1DCNN. Thus, the convolution operation is done on dilated format to get the required result. The given atrous based 1DCNN is implemented in multiple cascaded type. It means, the weight feature is given to the model by three times in parallel manner.
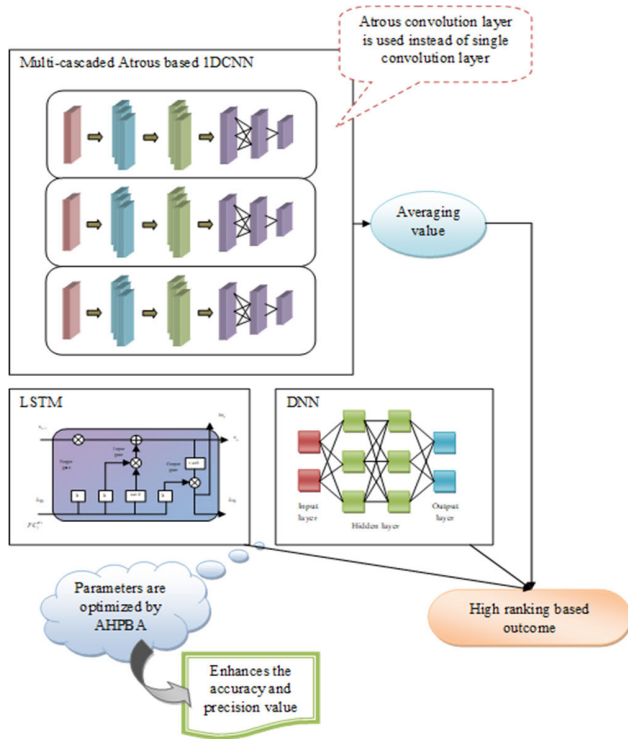
FIGURE 9. Block diagram of proposed MCA-DLS using parameter optimization of AHPBA.

Hence, the atrous based multi cascaded model processes the rich signal features to give the result for diagnosing purposes. During cascaded operation, the three scores are determined that is used for taking the average value of final result. Figure 9 elucidates the MCA-DLS for detecting the sleep apnea disorder. In the same way, the outcome of atrous based IDCNN, LSTM and DNN is used to compute the final expected result based on the high-ranking values. Though, it yields promising results, the parameters in these models may cause overfitting problem that mislead the detection process to provide the imprecise results, that is why multiple dropout layers are used in the classifiers. Further to improve the performance of this ENSEMBLE method, the hyperparameters are optimally determined by using AHPBA.

Hence, the objective function of AHPBAMCA-DLS is formulated using Equation (32).

$$
\begin{aligned}
&OF(2) \\
&= \underset{\{Hn^{1DCNN},Hn^{LSTM},Lr^{1DCNN},Lr^{DNN},Ep^{LSTM},Bs^{DNN}\}}{argmax} \left[ay + prn\right]
\end{aligned}
$$
(32)

Term, Hn^{1DCNN} and Hn^{LSTM} annotates the hidden neuron of 1DCNN and LSTM that lies in the range of (20 – 160). Then, the learning rate of 1DCNN and DNN is indicated by Lr^{1DCNN} and Lr^{DNN}, which contains the value of 0.1 to 0.9. Further, the epoch in LSTM is defined by Ep^{LSTM} varies from 50 to 220. Finally, the batch size of DNN is declared as Bs^{DNN} poses the value as 1 to 350.

Further, the term *ay* indicates the accuracy defined as the state or quality of representing the appropriate or precise value. It is calculated by Equation (33).

$$
ay = \frac{TPo + TNe}{TPo + TNe + FPo + FNe}
$$
(33)

Similarly, the precision *prn* computes the closeness rate of sleep apnea signals. It is expressed using Equation (34).

$$
prn = \frac{TPo}{TPo + FPo}
$$
(34)

In above two equations, the true positive and true negative is represented by TPo and TNe. Simultaneously, the false positive and negative rate is noted by FPo and FNe, respectively.

VI. DISCUSSION
A. EXPERIMENTAL SETUP
Two distinct ECG datasets were employed for the experimental process: 1. Apnea- Ecg Database, 2. MIT BIH database. Both these datasets have ECG signals of Apnea and Non apnea subjects. All the signals that are used for training are annotated by the physicians for minute by minute. Moreover, most of the signals are recorded for more than 5 hours of duration. The first dataset comprises of 100 Hz sampled signal whereas the second is of 250 Hz. Therefore the signals from the second dataset is decimated to 100 HZ for the unanimous usage. The complete model setup was implemented in python on a 16 GB intel Core i7-1360P supported with NVIDIA GeForce RTX 4090 GPU. For training 35 records from dataset1 and 12 records from dataset2 have been used. The remaining records were used for testing. The results reported here are the results of model with test set. The proposed algorithm has taken the total population size as10 and total iteration as 25. Both these values have been taken as trial-and-error method only. The parameters of the MCA DLS are as follows:

Multi cascaded Atrous based 1DCNN has three 1DCNN blocks which are connected to one another. The kernel size and the activation function are 5, Relu respectively for all the three blocks. The dilation rate was set as 2 and all the convolution layer is followed by a 1d Max Pool layer with a pooling size of 2. The number of filters in the three blocks were 32,64,128. After the three blocks 2 dense layers of 32 and 64 neurons were implemented serially with a softmax layer for calculating the probabilities.

LSTM has 128 Units with a dropout factor of 0.8 and a dense layer of 30 units with relu activation function with a dropout factor of 0.8 and three units of softmax layer to predict the class.

For deep neural networks, two hidden layers were used. The first one had 10 neurons. The second one was added to force the feature extraction by the network itself. This hidden layer reduces a 10 input to 5, therefore it has 5 neurons and the output layer had one neuron to classify the result. relu was used as the activation function here.
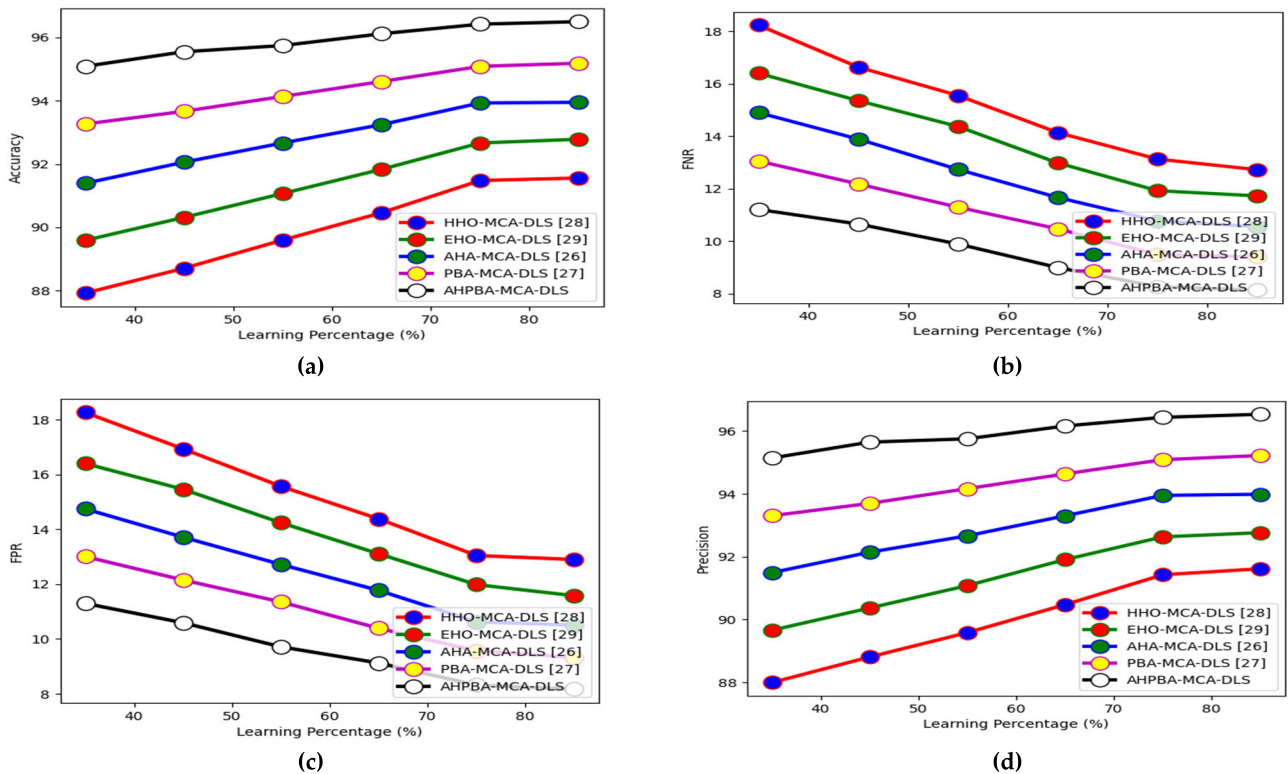
FIGURE 10. Performance analysis of suggested sleep apnea detection model compared over classical heuristic algorithms for dataset 1 regarding (a) Accuracy, (b) FNR, (c) FPR and (d) Precision.

Most of the parameters considered in the MCADLS classifiers are taken from literature and a subtle change has been made from experimentation to reduce the time consumption.

Diverse parameters like Accuracy, Sensitivity, Specificity, Precision, Negative Predictive Value (NPV), F1Score and Mathews Correlation Coefficient (MCC), False Positive Rate (FPR), False Negative Rate (FNR) and False Discovery Rate (FDR) for evaluating the performance. The algorithmic comparison was made with (Harris Hawks Optimization) HHO-MCA-DLS [52], (Elephant Herding Optimization) EHO-MCA-DLS [53], AHA-MCA-DLS [47] and PBA-MCA-DLS [48]. Meanwhile, the various deep learning models were taken as 1DCNN [33], LSTM [15], DNN [51] and Ensemble [54]. The proposed method's statistical power was calculated by testing the trained model with ten runs and the results were tabulated in table 4. The hyper parameters such as Hidden Neuron count is defined in the range of 20 – 160 for both 1DCNN and LSTM, Learning Rate ranges from 0.1-1 with a 0.1 incremental step size for both 1DCNN and DNN, Epoch size ranges from 50-220 for LSTM and the Batch size ranges from 1-350. The Ranges for all the hyper parameters have been taken based on literature and experimentation. The values of these parameters directly influence the rate of convergence of cost function as well as the quality of the solution. That is why these hyperparameters are chosen for optimization.

B. DIVERSE METRICS

In most of the works' accuracy was considered as a significant metric to evaluate a model's performance [55], but some more metrics are also to be considered as vital/supportive measures to evaluate the performance of a model [56]. Different measures considered in this work apart from accuracy and precision for evaluating the effectiveness of the model are described as follows.

FPR and FNR: The false positive rate provides the error value, in which the results are obtained incorrectly presence of signals. On the second hand, the false negative is used to determine the absence of apnea signal samples incorrectly actually when the signal is present.

$$FPR = \frac{FPo}{FPo + TNe} \quad (35)$$

$$FNR = \frac{FNe}{FNe + TPo} \quad (36)$$

Sensitivity and Specificity: Sensitivity is referred as the probability of actual positive rate and specificity is computed via possibility of negative rate.

$$Sensitivity = \frac{TPo}{TPo + FNe} \quad (37)$$

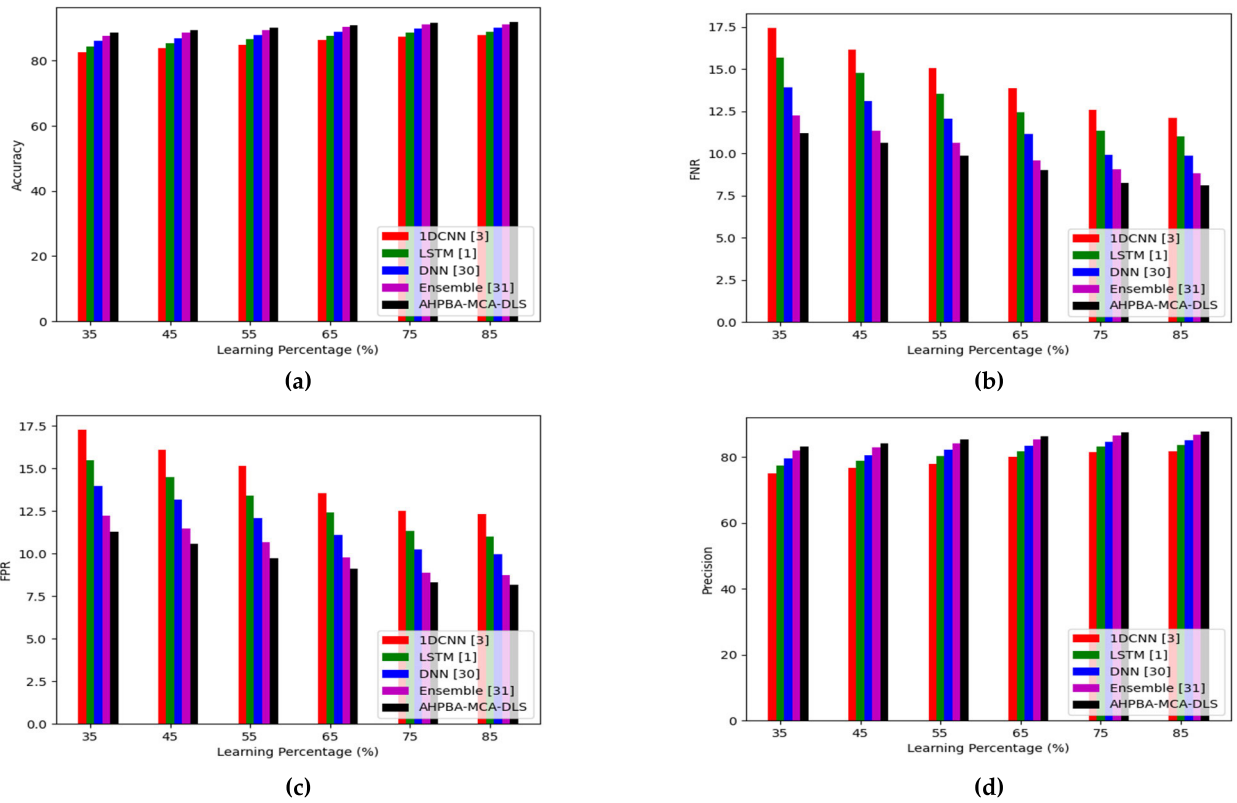$$Specificity = \frac{TNe}{TNe + FPo} \quad (38)$$

FIGURE 11. Performance analysis of suggested sleep apnea detection model compared over classical heuristic algorithms for dataset 1 regarding (a) Accuracy, (b) FNR, (c) FPR and (d) Precision.

FIGURE 12. Performance analysis of suggested sleep apnea detection model compared over classical heuristic algorithms for dataset 2 regarding (a) Accuracy, (b) FNR, (c) FPR and (d) Precision.
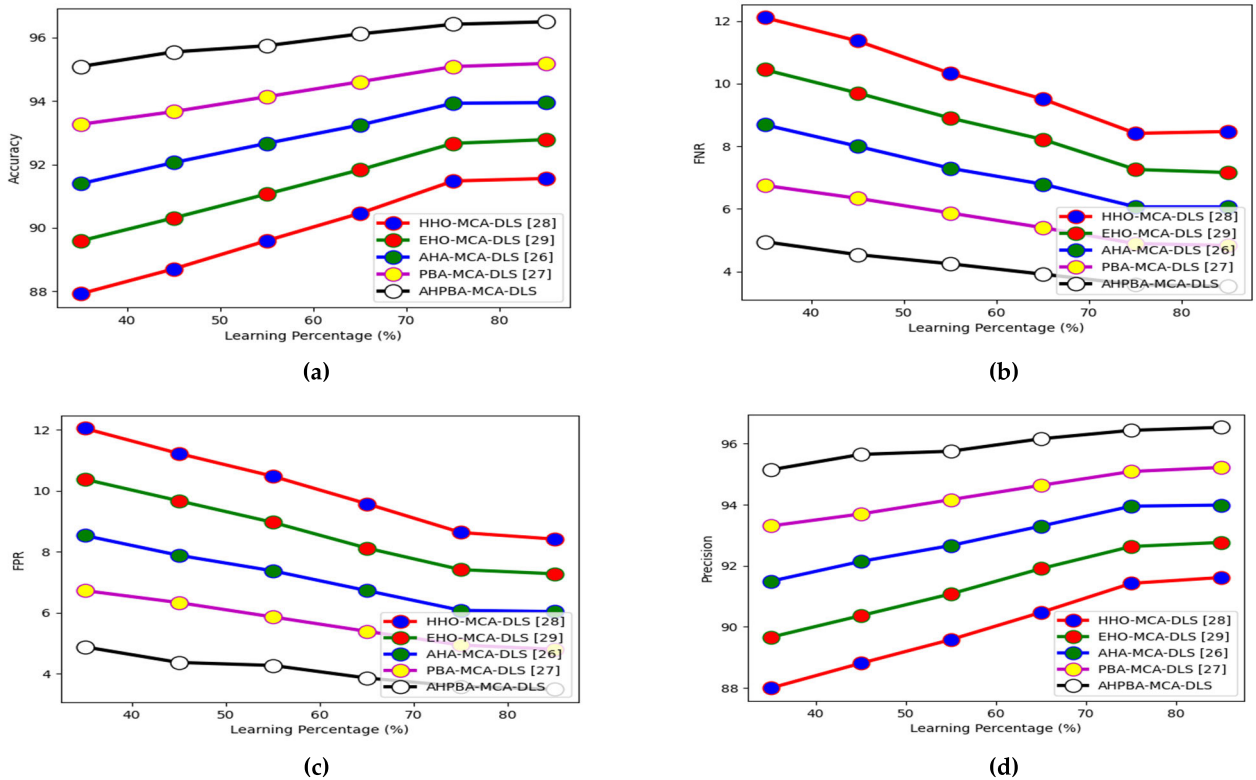
TABLE 1. Overall comparison of novel sleep apnea detection model using different optimization algorithms for two datasets.

Metrics	HHO-MCA-DLS	EHO-MCA-DLS	AHA-MCA-DLS	PBA-MCA-DLS	AHPBA-MCA-DLS
Dataset 1					
Accuracy	91.38095	92.6619	93.84286	95.138095	**96.42051**
Sensitivity	91.43174	92.60126	93.86926	95.13726	**96.40527**
Specificity	91.34892	92.70016	93.8262	95.13862	**96.39668**
Precision	90.25513	91.17081	92.64624	95.48622	**96.54402**
FPR	8.651083	7.299837	6.173798	4.861381	**3.603324**
FNR	8.568263	7.398744	6.13074	4.862735	**3.594731**
NPV	91.34892	92.70016	93.8262	95.13862	**96.39668**
FDR	13.04297	11.10848	9.441805	7.493416	**5.593731**
F1-Score	89.13826	90.70847	92.18401	93.80348	**95.3953**
MCC	0.820727	0.846976	0.871458	0.898284	**0.924543**
Dataset 2					
Accuracy	91.55634	92.60567	93.97862	95.07698	**96.4009**
Sensitivity	91.56721	92.56506	94.01291	95.08902	**96.36079**
Specificity	91.54542	92.64648	93.94416	95.06488	**96.44121**
Precision	91.58513	92.67385	93.97614	95.08902	**96.45515**
FPR	8.454581	7.353519	6.05584	4.935116	**3.558789**
FNR	8.432792	7.434944	5.987087	4.910976	**3.63921**
NPV	91.54542	92.64648	93.94416	95.06488	**96.44121**
FDR	8.414873	7.326151	6.023861	4.910976	**3.544849**
F1-Score	91.57617	92.61942	93.99452	95.08902	**96.40795**
MCC	0.831126	0.852113	0.879572	0.901539	**0.928018**

TABLE 2. Overall comparison of novel sleep apnea detection model using various deep classification techniques for two datasets.

Metrics	1DCNN	LSTM	DNN	Ensemble	AHPBA-MCA-DLS
Dataset 1					
Accuracy	90.87143	91.99048	93.21905	94.49524	**96.42051**
Sensitivity	90.82851	91.99803	93.20448	94.53404	**96.40527**
Specificity	90.8985	91.98571	93.22824	94.47076	**96.39668**
Precision	86.2924	87.86596	89.67192	91.51472	**94.40627**
FPR	9.101499	8.014289	6.771764	5.529238	**3.603324**
FNR	9.171488	8.00197	6.795519	5.465961	**3.594731**
NPV	90.8985	91.98571	93.22824	94.47076	**96.39668**
FDR	13.7076	12.13404	10.32808	8.485282	**5.593731**
F1-Score	88.50237	89.88453	91.40408	92.99988	**95.3953**
MCC	0.810146	0.833212	0.858524	0.884977	**0.924543**
Dataset 2					
Accuracy	90.80122	91.98784	93.29214	94.53761	**96.4009**
Sensitivity	90.70632	92.01722	93.28898	94.46292	**96.36079**
Specificity	90.89658	91.95832	93.29532	94.61266	**96.44121**
Precision	90.91979	91.99922	93.3255	94.62956	**96.45515**
FPR	9.103421	8.041683	6.70468	5.387338	**3.558789**
FNR	9.29368	7.982782	6.711015	5.537077	**3.63921**
NPV	90.89658	91.95832	93.29532	94.61266	**96.44121**
FDR	9.080212	8.000782	6.674496	5.370443	**3.544849**
F1-Score	90.81293	92.00822	93.30724	94.54617	**96.40795**
MCC	0.816027	0.839756	0.865842	0.890753	**0.928018**

F1-Score: It calculates the harmonic mean value of precision and recall.

$$F1Score = 2 * \frac{prn * re}{prn + re} \qquad (39)$$

FDR: It is defined as the ratio between false positive and total number of both true and false positive.

$$FDR = \frac{FPo}{TPo + FPo} \qquad (40)$$

NPV: The negative predictive rate is estimated by the ratio of true negative to the total value of true and false negative.

$$NPV = \frac{TNe}{TNe + FNe} \qquad (41)$$

MCC: It is evaluated by the difference between the classified value and actual value.

MCC
$$= \frac{TPo \times TNe - FPo \times FNe}{\sqrt{(TPo + FPo)(TPo + FNe)(TNe + FPo)(TNe + FNe)}} \qquad (42)$$

C. PERFORMANCE ANALYSIS ON SUGGESTED APNEA DETECTION FOR DATASET 1

While using dataset 1, Figure 10 shows the performance evaluation of sleep apnea detection over other heuristic approaches. Similarly, Figure 11 illustrates the evaluation for novel detection model using classical deep learning techniques with respect to four measures. The FNR analysis of recommended model is shown in Figure 10 (b) compared over classical algorithms. When the learning percentage is 55, the FNR value is yielded as 58.8%, 45%, 35.3% and 17.6% of HHO-MCA-DLS, EHO-MCA-DLS, AHA-MCA-DLS and PBA-MCA-DLS, correspondingly, which is greater than proposed AHPBA-MCA-DLS. Hence, the less false rate proves that it renders effective results for detecting the sleep apnea.

D. PERFORMANCE ANALYSIS ON SUGGESTED APNEA DETECTION FOR DATASET 2

Figure 12 & 13 represent the comparative analysis of enhanced apnea detection model compared with various heuristic and deep learning models using dataset 2. Figure 13 (c) shows the FPR analysis of novel method with respect to learning rate. At 65th learning percentage, the FPR of proposed model is acquired as 1.4% less than 1DCNN, 1.25% less than LSTM, 0.825% less than DNN and 0.475% less than Ensemble model, respectively. Thus, the method
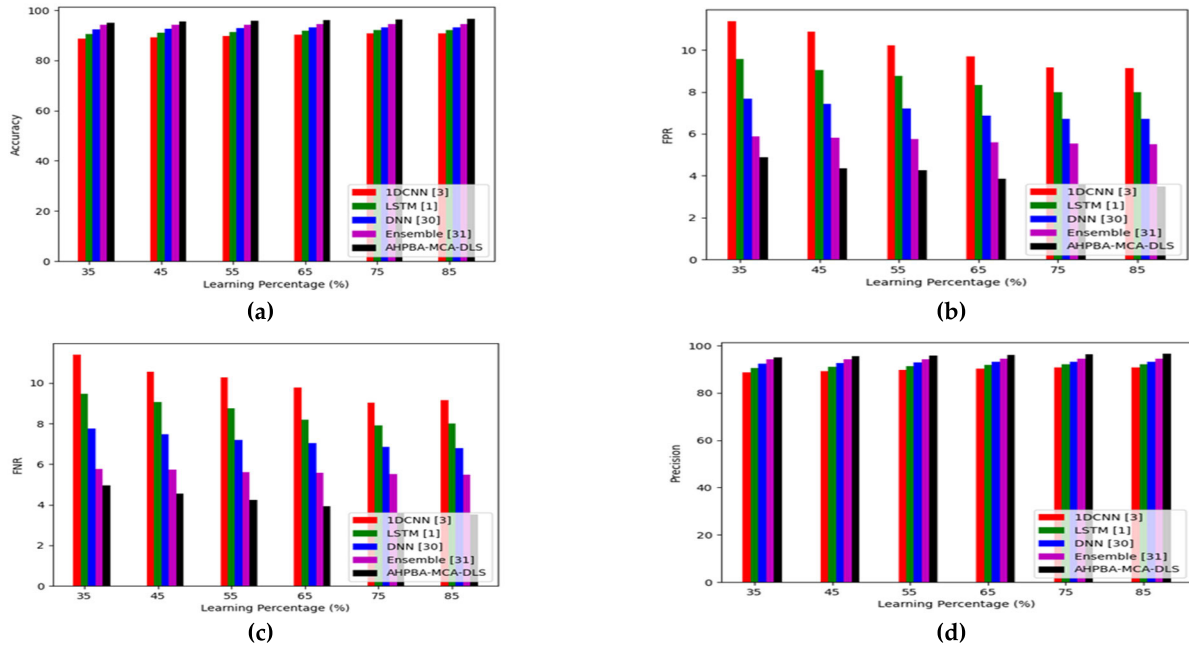
(a)

(b)

(c)

(d)

FIGURE 13. Performance analysis of suggested sleep apnea detection model compared over traditional deep learning model for dataset 2 with respect to (a) Accuracy, (b) FNR, (c) FPR and (d) Precision.
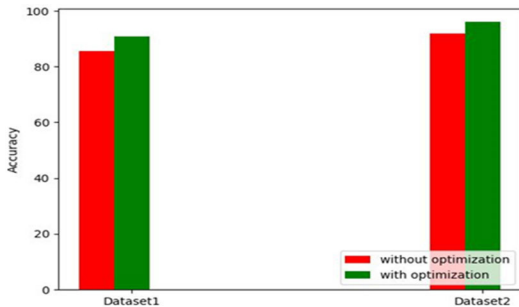

FIGURE 14. Accuracy of the MCADLS model with and without optimal feature selection.

attains fewer flaw rates to achieve more detection accuracy value.

E. OVERALL COMPARISON OF NOVEL DETECTION MODEL USING CLASSICAL ALGORITHMS

The overall estimation of proposed model with other algorithms is given in Table 1. The sensitivity value of proposed AHPBA-MCA-DLS is obtained as 5.15% higher than HHO-MCA-DLS, 4% more than EHO-MCA-DLS, 2.63% more than AHA-MCA-DLS and 1.31% higher than PBA-MCA-DLS, accordingly using dataset 1. Thus, the maximum true rate ensures that the model exhibits efficient performance.

F. OVERALL COMPARISON OF NOVEL DETECTION MODEL USING CLASSICAL LEARNING MODELS

Table 2 computes the overall value of proposed model and compares over distinct learning approaches. In dataset 2, the specificity value is obtained as 5.74% of 1DCNN, 4.64%

TABLE 3. Comparison of the proposed classifier with existing methods from literature with respect to dataset1.

Model	Accuracy (%)	Number of Features	Time (Seconds)
1DCNN [33]	87.6	1 (RR intervals – Multiple subsets at each level of CNN)	36
LSTM [15]	92.5	Deep features extracted using LSTM (31899 Samples.)	97
DNN [51]	92.1	7 (RR intervals – Mean, Median, Mode, SD, RMSSD, MAD, Inerquartile Range)	61
Proposed classifier (MCADLS)	94.43	Fused Features of 856700 Samples.	113
Proposed classifier with optimization. AHPBA - MCADLS	96.42	Fused Features of 856700 Samples.	126

of LSTM, 3.26% of DNN and 1.9% of Ensemble, which is inferior to suggested AHPBA-MCA-DLS. Hence, the results declared here proves that AHPBA enhances the detection accuracy value.

Table 3 and 4 shows the comparative reports of testing accuracy with number of features and time taken. The reported value for the literature works and the proposed model are acquired after implementing the same in our hardware using the signals in dataset1, as it is the most utilized dataset by many literatures for the detection of sleep apnea. The time reported in table 3 is the testing time taken to classify
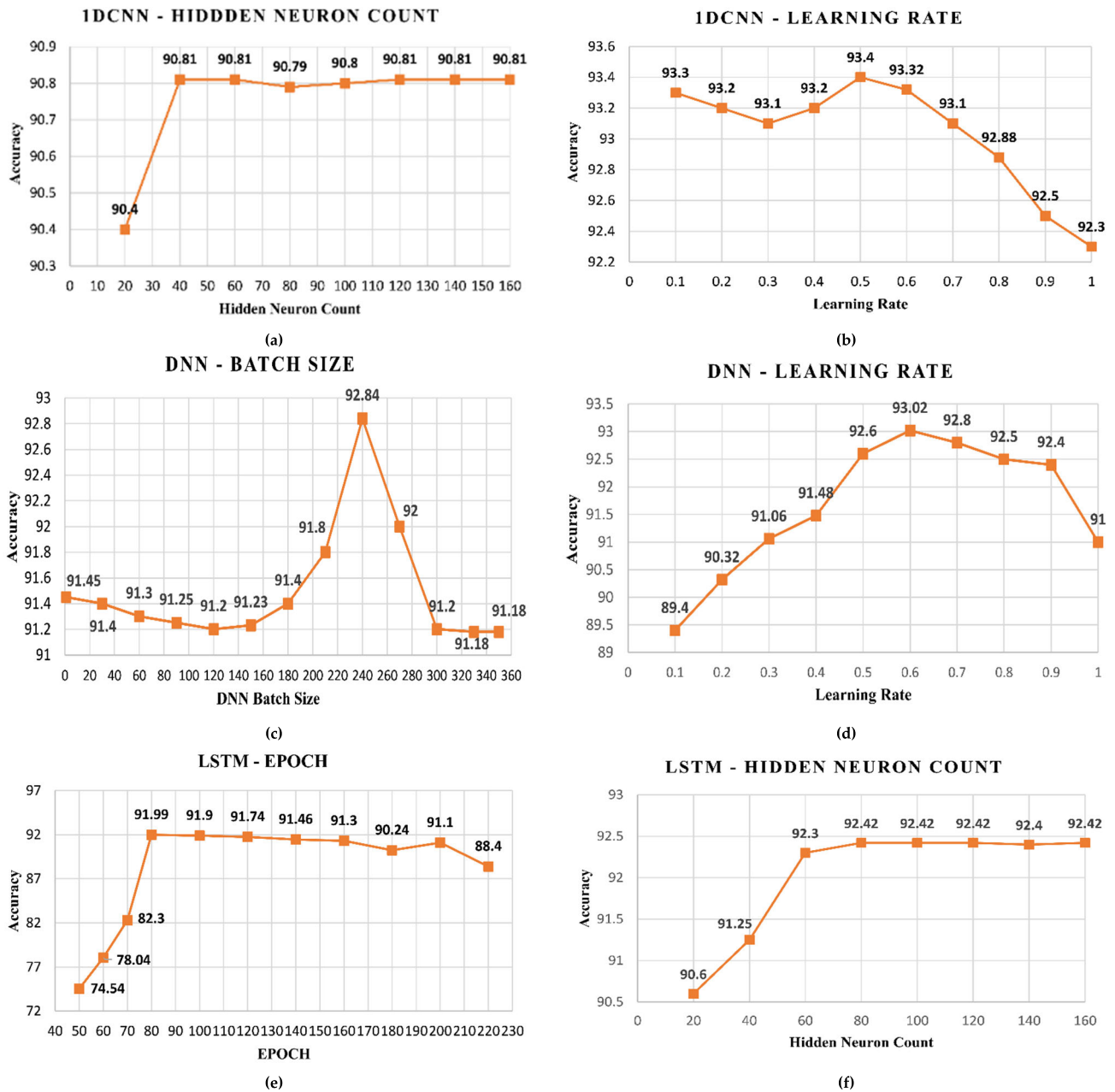
FIGURE 15. Chosen hyperparameters vs accuracy for dataset1.

the subject for a complete signal. Furthermore, the suggested cascaded classifier has excellent accuracy but also consumes significant processing time.

When it is further optimized, accuracy continues to rise, but testing times get longer. Therefore, there is a trade-off between accuracy and computational time. Compared to other optimization algorithm our proposed algorithm provides high accuracy with reasonable computation time.

This is the inevitable limitation of this work. To verify the reliability of this proposed model, the trained model on the first dataset is set to test the signals in the test set 10 times and the values of the most important metrics are given below.

From the above table it is evident that accuracy is 96.42051±0.505 for dataset1, similarly the same process was tried for dataset2, and the accuracy achieved is 96.4009±0.644 which is far better than the accuracies obtained from other models.

G. ANALYSIS OF FEATURES SELECTION PROCESS FOR TWO DATASETS

The accuracy obtained from MCADLS by giving inputs with and without weight optimization in feature selection is shown in Figure 14. From the graphical results, it is evident that the accuracy value gets increased by using the optimal selection of features and weights for both the datasets. Therefore,
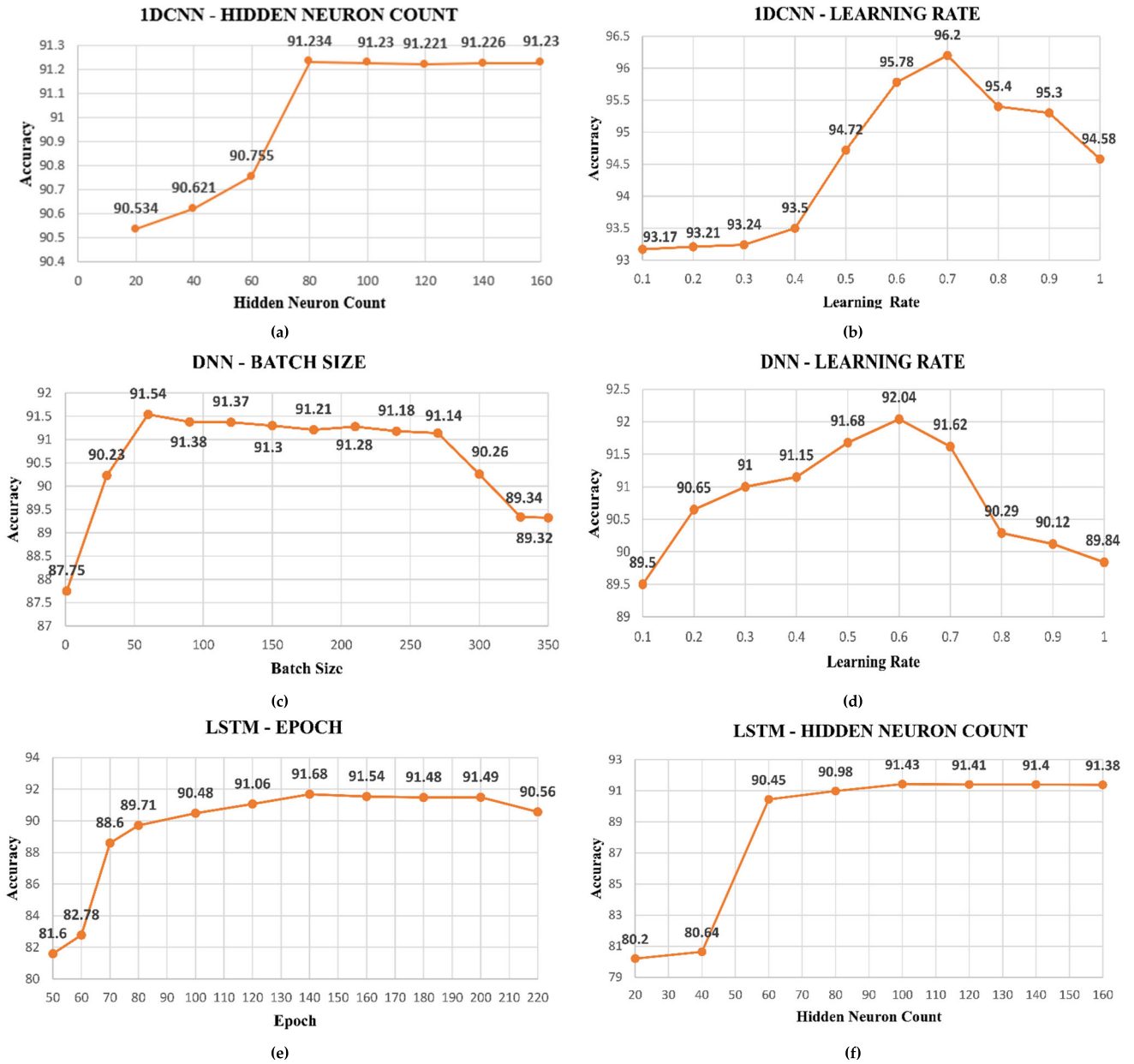
FIGURE 16. Chosen hyperparameters vs accuracy for dataset2.

feature selection with the help of this AHPBA optimization provides best results.

H. CLASSIFIER'S HYPER PARAMETER OPTIMIZATION

The optimizer optimizes the hidden neurons of 1DCNN and LSTM, learning rate of both 1DCNN and DNN, epochs in LSTM and batch size of DNN are optimally determined by using AHPBA to get the effective classification results. Figure 15 represents the relationship between various hyperparameters with respect to accuracy for dataset1. Using AHPBA all those hyperparameters are tuned and utilized for detecting OSA. Figure 15a represents the relationship between hidden neuron count and accuracy. The AHPBA

optimizes the hidden neuron count to get the maximum accuracy. Here it is around 40. Whereas for the second dataset it varies. It can be visualized in the figure 16a. Figure15b represents the relation between accuracy and the learning rate of 1DCNN. The accuracy is maximum when the learning rate is 0.5. Similarly Figure 15 c & d represents the relationship between batch size and learning rate of Deep Neural Network with respect to accuracy respectively.

The AHPBA helps to find the optimum value of both the hyper parameters to get the maximum accuracy. e & f of Figure15 represents the relationship between epoch and hidden neuron count with respect to accuracy for LSTM. The optimizer helps to find the optimal value of the above

TABLE 4. Comparison of the proposed optimized classifier with other existing optimization techniques with respect to dataset1.

Model	Accuracy (%)	Time (Seconds)
HHO - MCADLS	91.38	138
EHO - MCADLS	92.66	146
AHA-MCADLS	93.84	121
PBA-MCADLS	**95.14**	**133**
Proposed classifier with optimization. AHPBA - MCADLS	**96.42**	**126**

TABLE 5. Results of 10 runs on all 35-test data in dataset1.

Run	Specificity (%)	Sensitivity (%)	Accuracy (%)
1st	95.58286	97.7086	96.02866
2nd	96.79213	95.78546	95.2340
3rd	97.21030	95.10194	97.1230
4th	96.82779	97.42501	95.71802
5th	95.96537	97.02508	96.39946
6th	95.34795	95.9658	96.44156
7th	97.44521	95.99818	97.60702
8th	96.31053	95.38553	96.81236
9th	96.48263	96.84474	95.23658
10th	96.00103	96.81236	97.60444
Mean	**96.39668**	**96.40527**	**96.42051**
Standard Deviation	**0.58317**	**0.834453**	**0.50531**

mentioned hyperparameters which eventually improves the performance of classifiers in detecting the OSA. Figure 16 represents the relationship between various hyperparameters with respect to accuracy for dataset2. From the above figures it is very clear that optimization has played a very important role in improving the classifier's performance.

VII. CONCLUSION

This work has presented the adaptive detection model for diagnosing the sleep apnea. The proposed AHPBA-MCA-DLS provides better results compared to the recent existing optimization technique-based classifiers. While detecting OSA from the ECG signals in dataset1, AHPBA-MCA-DLS provides an accuracy of 96.4% which is 5.49% higher than HHO-MCA-DLS, 4.034% higher than EHO-MCA-DLS, 2.72% higher than AHA-MCA-DLS, 1.32% higher than PBA-MCA-DLS. Whereas AHPBA-MCA-DLS provides an accuracy of 96.4% while using ECG signals in dataset2 for OSA detection, which is 5.29% higher than HHO-MCA-DLS, 4.09% higher than EHO-MCA-DLS, 2.57% higher than AHA-MCA-DLS, 1.39% higher than PBA-MCA-DLS. Thus, on an average AHPBA-MCA-DLS provides an accuracy which is 5.39%, 4.06%, 2.65%, 1.35% greater than HHO-MCA-DLS, EHO-MCA-DLS, AHA-MCA-DLS, PBA-MCA-DLS respectively. To reduce the number of features from QRS analysis by denoising it, an auto encoder has been used. The usage of autoencoder has solved the dimensionality complexity to a major extent. In future work instead of autoencoder some more dimensionality reduction

algorithms can be used to enhance the feature selection process. Moreover, the fitness function of the AHPBA can be changed if needed for getting maximum accuracy and precision values. Without the optimization, the proposed MCADLS provides an accuracy of 94.49% & 94.53% for dataset1 and dataset2 respectively, which is slightly better than conventional classifiers. Here the spectral features are fused with the temporal features, that paves the way for utilising most of the meaningful features of the ECG signal in detection process, which only a very few has addressed. But those literatures didn't employ optimization for enhancing the result. Three best classifiers in business have been ensembled in this work, which are further optimized to get the solution very quickly and correctly. To prove the model's robustness, it has been tested with another dataset (mit-bih-polysonography) apart from ''The APNEA_ECG dataset'' and the results prove that this proposed model can be a robust one for different datasets. We have shown the reliability of the proposed model by testing it multiple times over two different datasets and the results have been tabulated in table 5. The inevitable limitation of this model is, at the cost of computational time the accuracy can be increased. Though the proposed model works efficiently well in classifying the apnea from non apnea in ECG signals, the computational time taken for cascaded approach is quite higher than the traditional individual one. It can be reduced in future by fine tuning the search space of the optimization algorithm.

REFERENCES

[1] X. Zhang, D. Huang, H. Li, Y. Zhang, Y. Xia, and J. Liu, "Self-training maximum classifier discrepancy for EEG emotion recognition," *CAAI Trans. Intell. Technol.*, pp. 1–12, Feb. 2023, doi: 10.1049/cit2.12174.

[2] Q. Zeng, B. Bie, Q. Guo, Y. Yuan, Q. Han, X. Han, M. Chen, X. Zhang, Y. Yang, M. Liu, P. Liu, H. Deng, and X. Zhou, "Hyperpolarized Xe NMR signal advancement by metal-organic framework entrapment in aqueous solution," *Proc. Nat. Acad. Sci. USA*, vol. 117, no. 30, pp. 17558–17563, Jul. 2020, doi: 10.1073/pnas.2004121117.

[3] L. Sun, M. Zhang, B. Wang, and P. Tiwari, "Few-shot class-incremental learning for medical time series classification," *IEEE J. Biomed. Health Informat.*, early access, Feb. 22, 2023, doi: 10.1109/JBHI.2023.3247861.

[4] Y. Zhuang, N. Jiang, and Y. Xu, "Progressive distributed and parallel similarity retrieval of large CT image sequences in mobile telemedicine networks," *Wireless Commun. Mobile Comput.*, vol. 2022, pp. 1–13, Jul. 2022, doi: 10.1155/2022/6458350.

[5] M. Liu, X. Zhang, B. Yang, Z. Yin, S. Liu, L. Yin, and W. Zheng, "Three-dimensional modeling of heart soft tissue motion," *Appl. Sci.*, vol. 13, no. 4, p. 2493, Feb. 2023, doi: 10.3390/app13042493.

[6] W. Dang, L. Xiang, S. Liu, B. Yang, M. Liu, Z. Yin, L. Yin, and W. Zheng, "A feature matching method based on the convolutional neural network," *J. Imag. Sci. Technol.*, vol. 67, no. 3, pp. 030402-1–030402-11, May 2023, doi: 10.2352/J.ImagingSci.Technol.2023.67.3.030402.

[7] N. Freedman, "Positive airway pressure treatment for obstructive sleep apnea," in *Principles and Practice of Sleep Medicine*. Amsterdam, The Netherlands: Elsevier, 2017, pp. 1125.e6–1137.e6.

[8] F. Wang, H. Wang, X. Zhou, and R. Fu, "A driving fatigue feature detection method based on multifractal theory," *IEEE Sensors J.*, vol. 22, no. 19, pp. 19046–19059, Oct. 2022, doi: 10.1109/JSEN.2022.3201015.

[9] F. Mendonça, S. S. Mostafa, A. G. Ravelo-García, F. Morgado-Dias, and T. Penzel, "A review of obstructive sleep apnea detection approaches," *IEEE J. Biomed. Health Informat.*, vol. 23, no. 2, pp. 825–837, Mar. 2019.

[10] P. de Chazal, C. Heneghan, E. Sheridan, R. Reilly, P. Nolan, and M. O'Malley, "Automatic classification of sleep apnea epochs using the electrocardiogram," in *Proc. Comput. Cardiol.*, Cambridge, U.K., vol. 27, 2002, pp. 745–748.

[11] M. Hafezi, N. Montazeri, S. Saha, K. Zhu, B. Gavrilovic, A. Yadollahi, and B. Taati, "Sleep apnea severity estimation from tracheal movements using a deep learning model," *IEEE Access*, vol. 8, pp. 22641–22649, 2020.

[12] H. Azimi, P. Xi, M. Bouchard, R. Goubran, and F. Knoefel, "Machine learning-based automatic detection of central sleep apnea events from a pressure sensitive mat," *IEEE Access*, vol. 8, pp. 173428–173439, 2020.

[13] Y. Zhuang, S. Chen, N. Jiang, and H. Hu, "An effective WSSENet-based similarity retrieval method of large lung CT image databases," *KSII Trans. Internet Inf. Syst.*, vol. 16, no. 7, pp. 2359–2376, 2022, doi: 10.3837/tiis.2022.07.013.

[14] B. Yang, Y. Li, W. Zheng, Z. Yin, M. Liu, L. Yin, and C. Liu, "Motion prediction for beating heart surgery with GRU," *Biomed. Signal Process. Control*, vol. 83, May 2023, Art. no. 104641, doi: 10.1016/j.bspc.2023.104641.

[15] A. Zarei, H. Beheshti, and B. M. Asl, "Detection of sleep apnea using deep neural networks and single-lead ECG signals," *Biomed. Signal Process. Control*, vol. 71, Jan. 2022, Art. no. 103125.

[16] K. Gupta, V. Bajaj, and I. A. Ansari, "OSACN-Net: Automated classification of sleep apnea using deep learning model and smoothed Gabor spectrograms of ECG signal," *IEEE Trans. Instrum. Meas.*, vol. 71, pp. 1–9, 2022.

[17] K. Li, W. Pan, Y. Li, Q. Jiang, and G. Liu, "A method to detect sleep apnea based on deep neural network and hidden Markov model using single-lead ECG signal," *Neurocomputing*, vol. 294, pp. 94–101, Jun. 2018.

[18] A. P. Razi, Z. Einalou, and M. Manthouri, "Sleep apnea classification using random forest via ECG," *Sleep Vigilance*, vol. 5, no. 1, pp. 141–146, Jun. 2021.

[19] H. Korkalainen, T. Leppänen, B. Duce, S. Kainulainen, J. Aakko, A. Leino, L. Kalevo, I. O. Afara, S. Myllymaa, and J. Töyräs, "Detailed assessment of sleep architecture with deep learning and shorter epoch-to-epoch duration reveals sleep fragmentation of patients with obstructive sleep apnea," *IEEE J. Biomed. Health Informat.*, vol. 25, no. 7, pp. 2567–2574, Jul. 2021.

[20] H. D. Nguyen, B. A. Wilkins, Q. Cheng, and B. A. Benjamin, "An online sleep apnea detection method based on recurrence quantification analysis," *IEEE J. Biomed. Health Informat.*, vol. 18, no. 4, pp. 1285–1293, Jul. 2014.

[21] X. Zhou and L. Zhang, "SA-FPN: An effective feature pyramid network for crowded human detection," *Int. J. Speech Technol.*, vol. 52, no. 11, pp. 12556–12568, Sep. 2022, doi: 10.1007/s10489-021-03121-8.

[22] C. Yang, X. Wang, and S. Mao, "Unsupervised detection of apnea using commodity RFID tags with a recurrent variational autoencoder," *IEEE Access*, vol. 7, pp. 67526–67538, 2019.

[23] S. H. Choi, H. Yoon, H. S. Kim, H. B. Kim, H. B. Kwon, S. M. Oh, Y. J. Lee, and K. S. Park, "Real-time apnea-hypopnea event detection during sleep by convolutional neural networks," *Comput. Biol. Med.*, vol. 100, pp. 123–131, Sep. 2018.

[24] U. Erdenebayar, Y. J. Kim, J.-U. Park, E. Y. Joo, and K.-J. Lee, "Deep learning approaches for automatic detection of sleep apnea events from an electrocardiogram," *Comput. Methods Programs Biomed.*, vol. 180, Oct. 2019, Art. no. 105001.

[25] D. Dey, S. Chaudhuri, and S. Munshi, "Obstructive sleep apnoea detection using convolutional neural network based deep learning framework," *Biomed. Eng. Lett.*, vol. 8, no. 1, pp. 95–100, Feb. 2018.

[26] H. B. Kwon, D. Son, D. Lee, H. Yoon, M. H. Lee, Y. J. Lee, S. H. Choi, and K. S. Park, "Hybrid CNN-LSTM network for real-time apnea-hypopnea event detection based on IR-UWB radar," *IEEE Access*, vol. 10, pp. 17556–17564, 2022.

[27] H. B. Kwon, S. H. Choi, D. Lee, D. Son, H. Yoon, M. H. Lee, Y. J. Lee, and K. S. Park, "Attention-based LSTM for non-contact sleep stage classification using IR-UWB radar," *IEEE J. Biomed. Health Informat.*, vol. 25, no. 10, pp. 3844–3853, Oct. 2021.

[28] S. Aswath and S. Valarmathi, "Obstructive sleep apnea severity prediction model GUI using anthropometrics," *Int. J. Electr. Electron. Eng.*, vol. 9, no. 12, pp. 134–144, Dec. 2022.

[29] H. Liu, H. Yuan, J. Hou, R. Hamzaoui, and W. Gao, "PUFA-GAN: A frequency-aware generative adversarial network for 3D point cloud upsampling," *IEEE Trans. Image Process.*, vol. 31, pp. 7389–7402, 2022, doi: 10.1109/TIP.2022.3222918.

[30] Q. Liao, H. Chai, H. Han, X. Zhang, X. Wang, W. Xia, and Y. Ding, "An integrated multi-task model for fake news detection," *IEEE Trans. Knowl. Data Eng.*, vol. 34, no. 11, pp. 5154–5165, Nov. 2022, doi: 10.1109/TKDE.2021.3054993.

[31] P. Chen, H. Liu, R. Xin, T. Carval, J. Zhao, Y. Xia, and Z. Zhao, "Effectively detecting operational anomalies in large-scale IoT data infrastructures by using a GAN-based predictive model," *Comput. J.*, vol. 65, no. 11, pp. 2909–2925, Nov. 2022, doi: 10.1093/comjnl/bxac085.

[32] F. Vaquerizo-Villar, D. Álvarez, L. Kheirandish-Gozal, G. C. Gutiérrez-Tobal, V. Barroso-García, E. Santamaría-Vázquez, F. D. Campo, D. Gozal, and R. Hornero, "A convolutional neural network architecture to enhance oximetry ability to diagnose pediatric obstructive sleep apnea," *IEEE J. Biomed. Health Informat.*, vol. 25, no. 8, pp. 2906–2916, Aug. 2021.

[33] Q. Shen, H. Qin, K. Wei, and G. Liu, "Multiscale deep neural network for obstructive sleep apnea detection using RR interval from single-lead ECG signal," *IEEE Trans. Instrum. Meas.*, vol. 70, pp. 1–13, 2021.

[34] F. R. Mashrur, M. S. Islam, D. K. Saha, S. M. R. Islam, and M. A. Moni, "SCNN: Scalogram-based convolutional neural network to detect obstructive sleep apnea using single-lead electrocardiogram signals," *Comput. Biol. Med.*, vol. 134, Jul. 2021, Art. no. 104532.

[35] Y. Wang, Z. Xiao, S. Fang, W. Li, J. Wang, and X. Zhao, "BI–directional long short-term memory for automatic detection of sleep apnea events based on single channel EEG signal," *Comput. Biol. Med.*, vol. 142, Mar. 2022, Art. no. 105211.

[36] F. Bozkurt, M. K. Uçar, C. Bilgin, and A. Zengin, "Sleep–wake stage detection with single channel ECG and hybrid machine learning model in patients with obstructive sleep apnea," *Phys. Eng. Sci. Med.*, vol. 44, no. 1, pp. 63–77, Mar. 2021.

[37] Z. Hu, L. Ren, G. Wei, Z. Qian, W. Liang, W. Chen, X. Lu, L. Ren, and K. Wang, "Energy flow and functional behavior of individual muscles at different speeds during human walking," *IEEE Trans. Neural Syst. Rehabil. Eng.*, vol. 31, pp. 294–303, 2023, doi: 10.1109/TNSRE.2022.3221986.

[38] S. Yang, Q. Li, W. Li, X. Li, and A.-A. Liu, "Dual-level representation enhancement on characteristic and context for image-text retrieval," *IEEE Trans. Circuits Syst. Video Technol.*, vol. 32, no. 11, pp. 8037–8050, Nov. 2022, doi: 10.1109/TCSVT.2022.3182426.

[39] A.-A. Liu, Y. Zhai, N. Xu, W. Nie, W. Li, and Y. Zhang, "Region-aware image captioning via interaction learning," *IEEE Trans. Circuits Syst. Video Technol.*, vol. 32, no. 6, pp. 3685–3696, Jun. 2022, doi: 10.1109/TCSVT.2021.3107035.

[40] Y. Shi, J. Hu, Y. Wu, and B. K. Ghosh, "Intermittent output tracking control of heterogeneous multi-agent systems over wide-area clustered communication networks," *Nonlinear Anal., Hybrid Syst.*, vol. 50, Nov. 2023, Art. no. 101387, doi: 10.1016/j.nahs.2023.101387.

[41] Y. Shen, N. Ding, H.-T. Zheng, Y. Li, and M. Yang, "Modeling relation paths for knowledge graph completion," *IEEE Trans. Knowl. Data Eng.*, vol. 33, no. 11, pp. 3607–3617, Nov. 2021, doi: 10.1109/TKDE.2020.2970044.

[42] B. Cheng, M. Wang, S. Zhao, Z. Zhai, D. Zhu, and J. Chen, "Situation-aware dynamic service coordination in an IoT environment," *IEEE/ACM Trans. Netw.*, vol. 25, no. 4, pp. 2082–2095, Aug. 2017, doi: 10.1109/TNET.2017.2705239.

[43] L. Sun, J. Liang, C. Zhang, D. Wu, and Y. Zhang, "Meta-transfer metric learning for time series classification in 6G-supported intelligent transportation systems," *IEEE Trans. Intell. Transp. Syst.*, early access, Mar. 6, 2023, doi: 10.1109/TITS.2023.3250962.

[44] S. Srimathi, G. Yamuna, and R. Nanmaran, "Neural networks based cancer classification model using CT-PET fused images," in *Communications in Computer and Information Science*. Singapore: Springer, 2019, pp. 104–116.

[45] S. Srimathi, G. Yamuna, and R. Nanmaran, "An efficient cancer classification model for CT/MRI/PET fused images," *Current Med. Imag. Formerly Current Med. Imag. Rev.*, vol. 17, no. 3, pp. 319–330, Apr. 2021.

[46] S. Aswath, N. Bharanidharan, R. S. Valarmathi, and H. Rajaguru, "Modified spotted hyena optimizer based leukemia microscopic images classification," in *Proc. 6th Kuala Lumpur Int. Conf. Biomed. Eng.*, Cham, Switzerland: Springer, 2022, pp. 123–131.

[47] W. Zhao, L. Wang, and S. Mirjalili, "Artificial hummingbird algorithm: A new bio-inspired optimizer with its engineering applications," *Comput. Methods Appl. Mech. Eng.*, vol. 388, Jan. 2022, Art. no. 114194.

[48] N. A. Kallioras, N. D. Lagaros, and D. N. Avtzis, "Pity beetle algorithm—A new Metaheuristic inspired by the behavior of bark beetles," *Adv. Eng. Softw.*, vol. 121, pp. 147–166, Jul. 2018.

[49] D. Jiang, Y. Ma, and Y. Wang, "A multi-scale parallel convolutional neural network for automatic sleep apnea detection using single-channel EEG signals," in *Proc. 11th Int. Congr. Image Signal Process., Biomed. Eng. Informat. (CISP-BMEI)*, Beijing, China, Oct. 2018, pp. 1–5.

[50] S. S. Mostafa, F. Mendonca, F. Morgado-Dias, and A. Ravelo-Garcia, "SpO2 based sleep apnea detection using deep learning," in *Proc. IEEE 21st Int. Conf. Intell. Eng. Syst. (INES)*, Larnaca, Cyprus, Oct. 2017, pp. 000091–000096.

[51] M. Alsalamah, S. Amin, and V. Palade, "Clinical practice for diagnostic causes for obstructive sleep apnea using artificial intelligent neural networks," in *Emerging Technologies in Computing* (Lecture Notes of the Institute for Computer Sciences, Social Informatics and Telecommunications Engineering), vol. 200. Cham, Switzerland: Springer, 2018.

[52] A. A. Heidari, S. Mirjalili, H. Faris, I. Aljarah, M. Mafarja, and H. Chen, "Harris hawks optimization: Algorithm and applications," *Future Gener. Comput. Syst.*, vol. 97, pp. 849–872, Aug. 2019.

[53] N. K. Meena, J. Yang, and A. Slowik, "Elephant herding optimization," in *Swarm Intelligence Algorithms*, 1st ed. Boca Raton, FL, USA: Taylor & Francis, 2020, pp. 149–162.

[54] M. J. Rahman, R. Mahajan, and B. I. Morshed, "Severity classification of obstructive sleep apnea using only heart rate variability measures with an ensemble classifier," in *Proc. IEEE EMBS Int. Conf. Biomed. Health Informat. (BHI)*, Las Vegas, NV, USA, Mar. 2018, pp. 259–272.

[55] S. Aswath, C. M. S. Kumar, K. Reethi, B. Deepthi, K. Chikitha, and S. Rupesh, "Enhancing the performance of classifiers in detecting abnormalities in medical data using nature inspired optimization techniques," in *Proc. Int. Conf. Advancement Technol. (ICONAT)*, Jan. 2022, pp. 1–7.

[56] A. Hekmatmanesh, M. Mikaeili, K. Sadeghniiat-Haghighi, H. Wu, H. Handroos, R. Martinek, and H. Nazeran, "Sleep spindle detection and prediction using a mixture of time series and chaotic features," *Adv. Electr. Electron. Eng.*, vol. 15, no. 3, pp. 435–447, Oct. 2017.

VALARMATHI RAVICHANDRAN SHANMUGA SUNDARAM (Member, IEEE) received the B.E. and M.E. degrees in applied electronics from Bharathiar University, Coimbatore, in April 1989 and January 2000, respectively, and the Ph.D. degree in the area of biometrics from Anna University, Chennai, in 2009. She is currently a Professor with the Department of Electronics and Communication Engineering, Vel Tech Rangarajan Dr. Sagunthala R&D Institute of Science and Technology, Chennai. She has more than 30 years of teaching experience in various engineering colleges and 19 years of research experience. She has produced 12 Ph.D. graduates till date. She has published 130 research articles in the refereed international and national journals and 106 research papers in international and national conferences in the fields of image processing, biometrics, networks, VLSI, and cloud computing. She is a Life Member of the Indian Society for Technical Education (ISTE), a fellow of the Institution of Electronics and Telecommunication Engineers (IETE), and a member of the Institution of Engineers (IE).
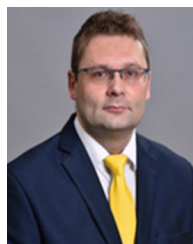
SELVARAJ ASWATH (Member, IEEE) received the B.E. and M.E. degrees from Anna University, Chennai, in 2010 and 2012, respectively. He is currently a Research Scholar with the Department of Electronics and Communication Engineering, Vel Tech Rangarajan Dr. Sagunthala R&D Institute of Science and Technology, Chennai, where he is also an Assistant Professor with the Department of Electronics and Communication Engineering. He is also a member of Signal Processing Society. He has more than ten years of teaching experience in various engineering colleges. He has published 20 research articles in the refereed international journals and conferences.

MIROSLAV MAHDAL is currently the Vice-Dean for Science, Research and Doctoral Studies with the Faculty of Mechanical Engineering, VSB-Technical University of Ostrava, and an Associate Professor with the Department of Control Systems and Instrumentation. His research interests include the control of mechatronic systems, control systems, automatic control theory, wireless technologies, artificial intelligence, cloud computing, optimization methods, and the programming of control systems. He has nearly more than 80 articles to his credit.

• • •